

Rapporti tecnici INGV

**Improved instruments for
volcanic plume observation for
monitoring purpose: Solfatara and
Vulcano island preliminary results**

349



Direttore Responsabile

Silvia MATTONI

Editorial Board

Luigi CUCCI - Editor in Chief (INGV-RM1)

Raffaele AZZARO (INGV-CT)

Mario CASTELLANO (INGV-NA)

Viviana CASTELLI (INGV-BO)

Rosa Anna CORSARO (INGV-CT)

Mauro DI VITO (INGV-NA)

Marcello LIOTTA (INGV-PA)

Mario MATTIA (INGV-CT)

Milena MORETTI (INGV-CNT)

Nicola PAGLIUCA (INGV-RM1)

Umberto SCIACCA (INGV-RM2)

Alessandro SETTIMI (INGV-RM2)

Salvatore STRAMONDO (INGV-CNT)

Andrea TERTULLIANI (INGV-RM1)

Aldo WINKLER (INGV-RM2)

Segreteria di Redazione

Francesca Di Stefano - Referente

Rossella Celi

Tel. +39 06 51860068

redazionecen@ingv.it

in collaborazione con:

Barbara Angioni (RM1)

REGISTRAZIONE AL TRIBUNALE DI ROMA N.173 | 2014, 23 LUGLIO

© 2014 INGV Istituto Nazionale di Geofisica e Vulcanologia

Rappresentante legale: Carlo DOGLIONI

Sede: Via di Vigna Murata, 605 | Roma



Rapporti tecnici INGV

IMPROVED INSTRUMENTS FOR VOLCANIC PLUME OBSERVATION FOR MONITORING PURPOSE: SOLFATARA AND VULCANO ISLAND PRELIMINARY RESULTS

Malvina Silvestri¹, Jorge Andres Diaz², Fabio Vita³, Massimo Musacchio¹, Jochen Puchalla⁴, Sergio Falcone⁵, Maria Fabrizia Buongiorno¹, Fawzi Doumaz¹, Kenneth Wright⁶

¹INGV (Istituto Nazionale di Geofisica e Vulcanologia, Centro Nazionale Terremoti)

²GASLAB, CICANUM (Universidad de Costa Rica, San José, Costa Rica)

³INGV (Istituto Nazionale di Geofisica e Vulcanologia, Sezione di Palermo)

⁴INFICON GmbH (Köln, Germany)

⁵INGV (Istituto Nazionale di Geofisica e Vulcanologia, Sede di Rende)

⁶INFICON (Syracuse, New York 13057, United States)

349

Index

Introduction	7
1. Test sites	7
2. The field campaign	7
2.1 <i>In situ</i> gas measurements	7
2.1.1 Helium measurements (vulcan t-guard).....	8
2.1.2 CO ₂ , SO ₂ , H ₂ S measurements (ntx minigas).....	9
2.1.3 Multigas analysis using portable mass spectrometers (uas-ms-mph and uas-ms-xpr3 systems).....	16
2.1.4 Drones and dem test on vulcano crater	18
2.2 SO ₂ measurement using lp-active doas and scanning doas	19
2.2.1 SO ₂ measurements at la solfatara and at vulcano island	19
2.2.2 Configuration of lp-doas measurements at la solfatara vulcano	20
2.2.3 Configuration of lp-doas measurements at vulcano island	21
2.2.4 Configuration of scanning doas measurements at vulcano island	23
2.3 Photometric measurement	25
2.4 Thermal measurements	27
2.5 Radiance and reflectance measures	29
30 Satellite Data	36
3.1 Landsat 8 Data	36
Conclusions	38
Acknowledgements	39
References	39

Introduction

This report describes the methodology, instruments and findings of the field campaign which took place at the beginning of September 2015 in Solfatara (Naples) and Vulcano Island. The campaign was held in order to test miniaturized instruments developed for NASA under Research Opportunities in Space and Earth Science (ROSES), and was part of a framework of monitoring activities on active volcanoes. It followed a first campaign held in Naples on the 30th and 31th October 2014 and described in Silvestri et al., [2015]. In the first campaign miniaturized multi-gas instruments for the CO₂, H₂S and SO₂ measurements were tested for the first time on Solfatara site and some of the results were reported in Silvestri et al., 2015. During these campaigns, measurements of *in situ* gaseous emissions have been collected using different instruments also mounted on drones. To complete the analysis conducted during the Vulcano campaign, some results using the spectro-radiometer ASD FieldSpec and thermal camera of the optical laboratory of “Unità Funzionale Dati satellitari per l’osservazione della Terra” (UF8) of INGV section of CNT are also reported. Moreover, the Vulcano island field campaign has been organized considering also the satellite data acquisitions from TERRA ASTER and LANDSAT 8. Both satellites data will be used to compare their measurements with the *in situ* data collected as regards temperature.

1. Test sites

The Solfatara of Pozzuoli, near Naples, is part of the Campi Flegrei volcanic complex that contains a fumarolic field more or less extended, whose activity is mainly characterized by the focused release of steam and gases with high sulphur component. The site is well known and studied, thanks to recurring campaigns for monitoring local volcanic activity. The last field campaign, carried out on October 2014 in collaboration with INGV staff (Rome and Naples), the University of Costa Rica and Jet Propulsion Laboratory of the California Institute of Technology (Pasadena, California) has offered the opportunity to start of testing miniaturized instruments for measuring SO₂, CO₂ and H₂S contents [Silvestri et al., 2015]. A new campaign was organized on 31st August and 1st September 2015 at Solfatara, while a successive campaign has been planned at Vulcano Island (from 1st to 7th September) in order to verify the instrument portability in areas without easy access.

With regards to Vulcano Island, its two overlapping calderas, the 2.5-km-wide Caldera del Piano on the SE and the 4-km-wide Caldera della Fossa on the NW, were formed at about 100,000 and 24,000-15,000 years ago, respectively, with volcanism migrating to the north over time. La Fossa cone, which was active throughout the Holocene and where most of the historical eruptions occurred, occupies the 3-km-wide Caldera della Fossa at the NW end of the elongated 3 x 7 km island. The latest Vulcano eruption consisted of explosive activity that occurred from 1898 to 1900 from the Fossa cone. Since then, the volcano never ceased to show signs of its activity and still today different phenomena are observed, including numerous fumaroles, which strongly characterize the environment as well as the landscape and the intense fragrance of the island, which reminds us of its uniqueness. The hot springs along the beach near “Porto di Levante” are particularly striking: they are the result of water and mud being heated by volcanic/hydrothermal gases which are released by low-flux fumaroles. The thermal springs on Vulcano Island are a unique phenomenon unto themselves and attract thousands of visitors each year. Over the past fifty years, visitors have benefitted from the therapeutic effects of mud and thermal baths on Vulcano.

2. The field campaign

2.1 *In situ* gas measurements

A series of new instruments for *in situ* gas measurement were used in the 2015 Solfatara-Vulcano campaign to test new techniques and methods to collect fresh information about the chemical composition of the gaseous volcanic emissions. The instruments include a miniature Gas Analysis System: the miniGAS NTX, which is an updated version of the Dragon and Alpha NTX payloads suites tested in 2014 and designed for drone integration; two unmanned aerial vehicle mass spectrometer systems: the UAS-MS-XPR3 and UAS-MS-MPH designed for simultaneous *in situ* gas analysis from ppm to 100% level concentration measurements using mass spectrometry in a backpack integrated option; and a helium monitor system: the Vulcan T-Guard, an high sensitive helium leak detector modified and adapted to monitor natural helium emissions from volcanic sites.

2.1.1 Helium Measurements (Vulcan T-Guard)

The INFICON T-Guard (Figure 1) is a sensor with a helium-permeable membrane to detect helium. The correct helium level is determined by a pressure variation in front of the sensor. This sensor delivers the sensitivity and speed helium leak detectors are known for, at a cost similar to pressure decay systems. T-Guard works with simple chambers at atmospheric pressure, so there is no need for costly and complex high vacuum chambers and pumps. The sensor offers a low-price helium leak test, which is 100 times more sensitive than pressure decay systems - and temperature independent - and up to 1,000 times more sensitive than the water bath bubble test. Unlike traditional detectors, the T-Guard sensor does not use a turbomolecular pump to measure the helium partial pressure; it uses a patented helium permeable membrane chip combined with a penning gauge. Moreover it does not need high vacuum to measure tiny concentrations of helium accurately. The measurements are also highly repeatable, even with large, warm or humid test objects.



Figure 1. Vulcan T-Guard sensor, produced by INFICON.

Via the sensor signal variation and the sensor sensitivity one can calculate the absolute helium level with an accuracy of 0.2 ppm. For the Solfatara-Vulcano campaign, a portable system was developed (the Vulcan version) in which the T-Guard is controlled by a Raspberry Pi mini-PC with its own Wi-Fi network to access and download the data. The air inlet to T-Guard is a flexible hose which can be positioned and/or extended to reach the desired measurement point. The software generates one data point per minute in its graph and produces Excel-data file as output. The whole setup is able to run on 5 conventional USB power banks for a few hours.

T-Guard was able to measure up to 7 ppm of Helium at Solfatara volcano and up to 450 ppm of Helium on Vulcano island (Figure 2), but it needs more testing and calibration to validate this measurements.

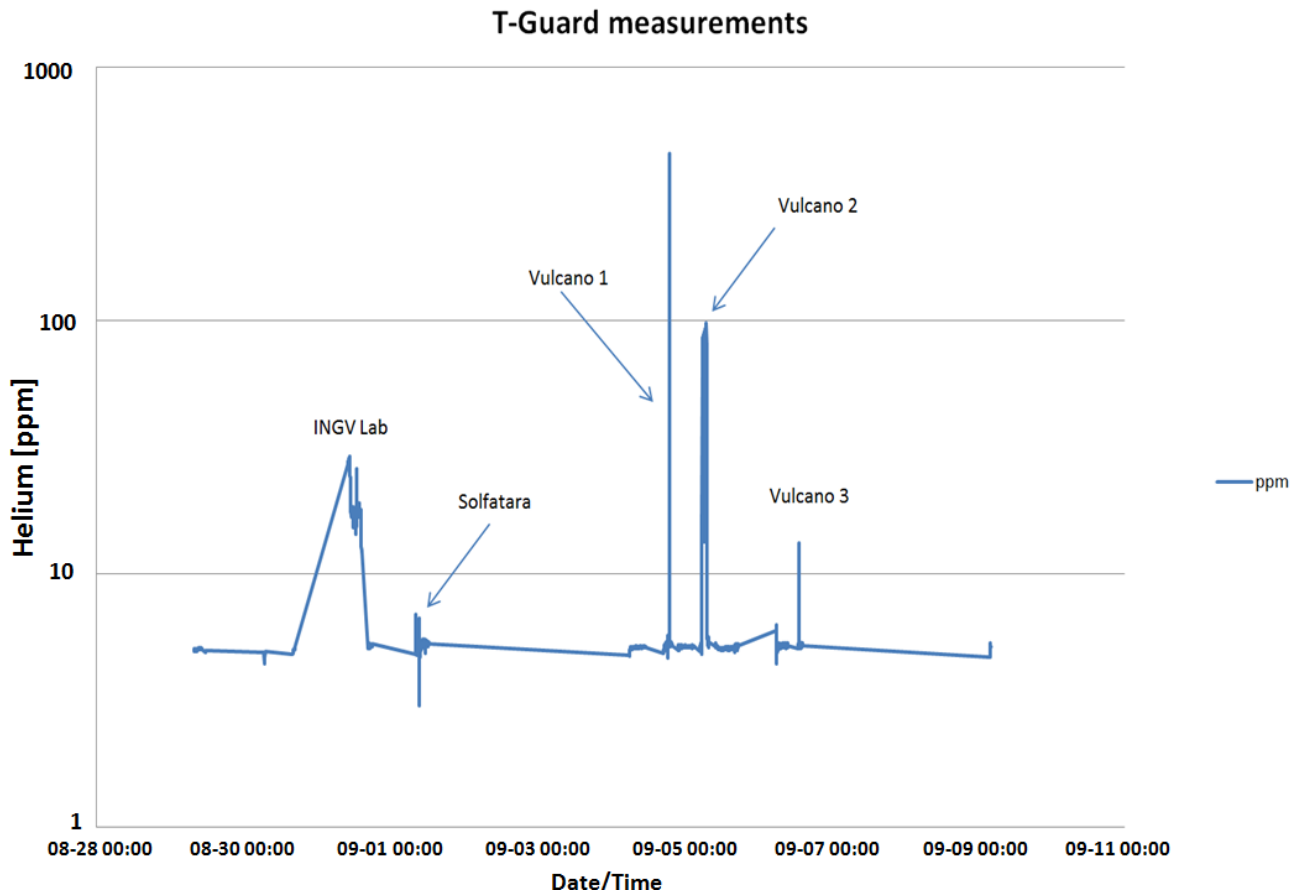


Figure 2. T-Guard helium measurements collected during the field campaigns.

2.1.2 CO₂, SO₂, H₂S measurements (NTX MiniGAS)

The NTX MiniGAS (Figure 3) is a multisensor instrument based on an Arduino platform developed by Dr. Diaz lab at the University of Costa Rica and includes commercial of the shelf (COTS) temperature, pressure, relative humidity sensor, SO₂ and H₂S electrochemical sensors from City Technologies, a non-dispersing near infrared CO₂ sensor, Arduino GPS sensor, onboard data storage and telemetry via Xbee Pro 900 Mhz antennas. Earlier versions: the Dragon and Alpha MiniGAS systems has been flight tested in Costa Rica within the Turrialba volcano plume onboard the VECTOR WING 100 UAV [Pieri et al., 2013] and tethered balloon airborne platforms, generating real time 3D gas concentration plots of the active volcanic plumes. *In situ* sampling with the MiniGAS is achieved by injecting an airstream into the multi sensor platform with a very small displacement pump (1.2 Lpm) to generate a concentration profile. The NTX MiniGas is a newer version with improved CO₂ sensor (NG Gascard from Edinburg Instruments), improved Arduino mainboard and software-hardware interface and was deployed for the Solfatara-Vulcano 2015 campaign to characterize the fumarolic site. The measurements were conducted either by hand carrying the instrument into the fumaroles (“sampling walk”) or flying two different Drones (DJI S800 Hexacopter and Italdrone E-EPIC8 Octocopter) over the fumarolic sites.

Examples of 3D volcanic gases measurements acquired on the Solfatara (Figure 4 and Figure 5) and and Vulcano (Figure 6 - Figure 10) are reported here.



Figure 3. The NTX MiniGAS instrument produced by Gas Lab, CICANUM, Universidad de Costa Rica.

In the next figures some preliminary results of CO₂, H₂S and SO₂ concentrations are reported.

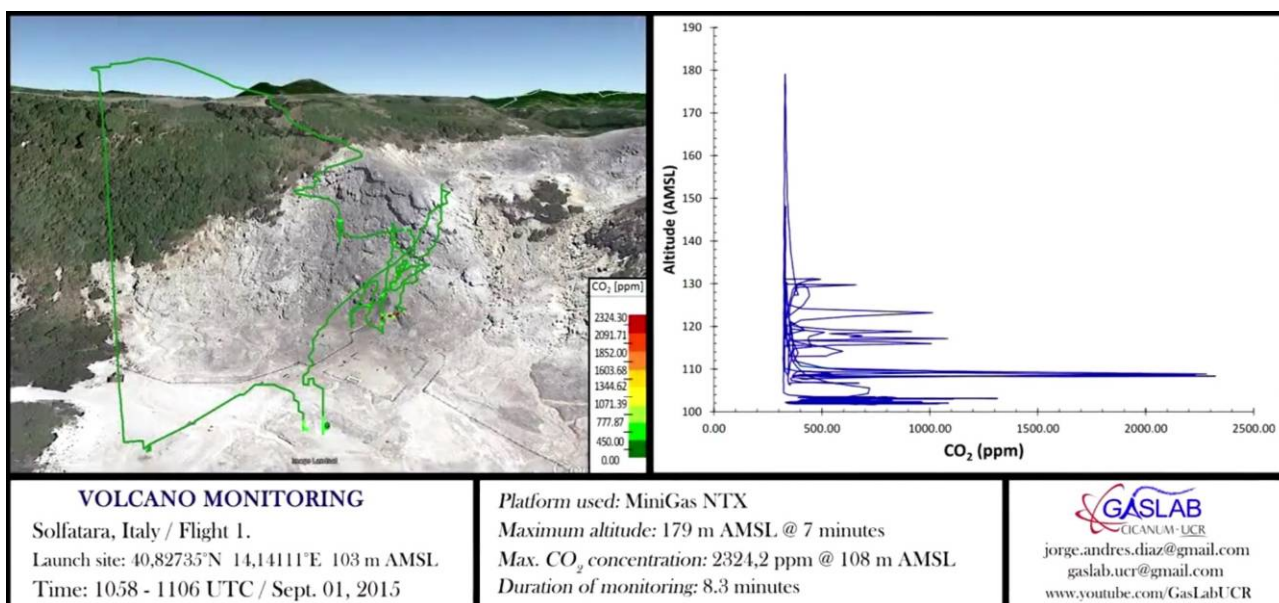


Figure 4. 3D view of CO₂ concentration on Solfatara area. On the right picture: trend of the concentration of CO₂ as a function of altitude. Trajectories in Google Earth™ images are colour-coded according to the legend on the left image. The measurements have been collected with the Italdrone Octocopter.

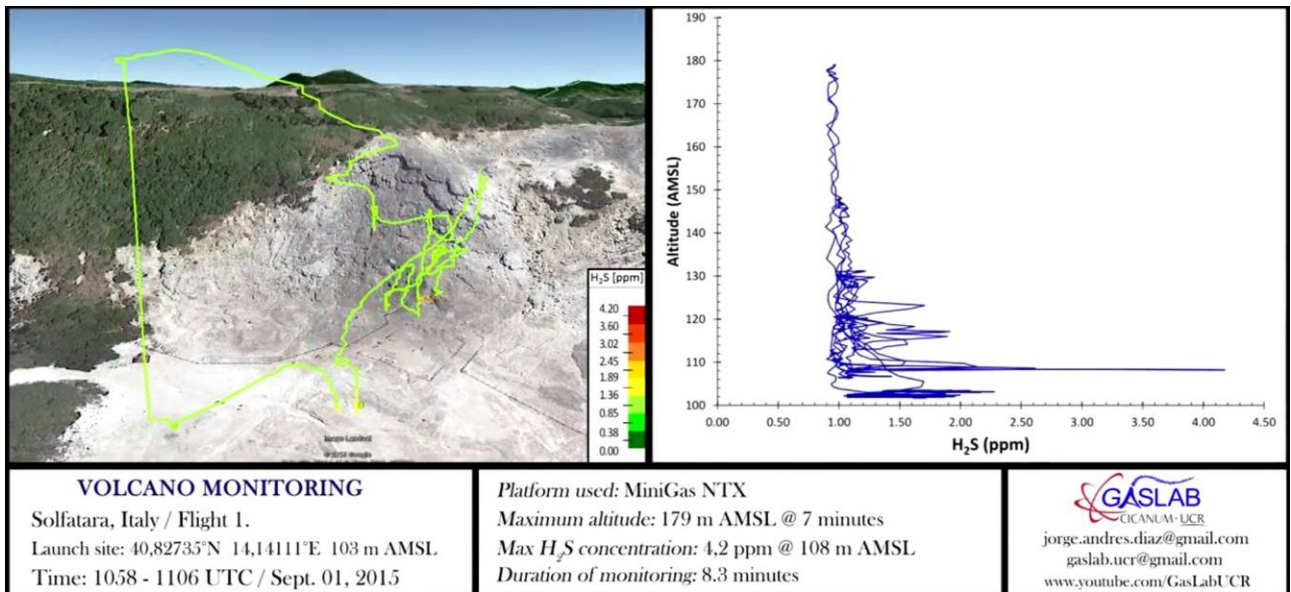


Figure 5. 3D view of H_2S concentration on Solfatara area. On the right picture: trend of the concentration of H_2S as a function of altitude. Trajectories in Google Earth™ images are colour-coded according to the legend on the left image. The measurements have been collected with Italdrone Octocopter.

The volcanic gases measurements have been collected using Hexacopter and Octocopter drones.

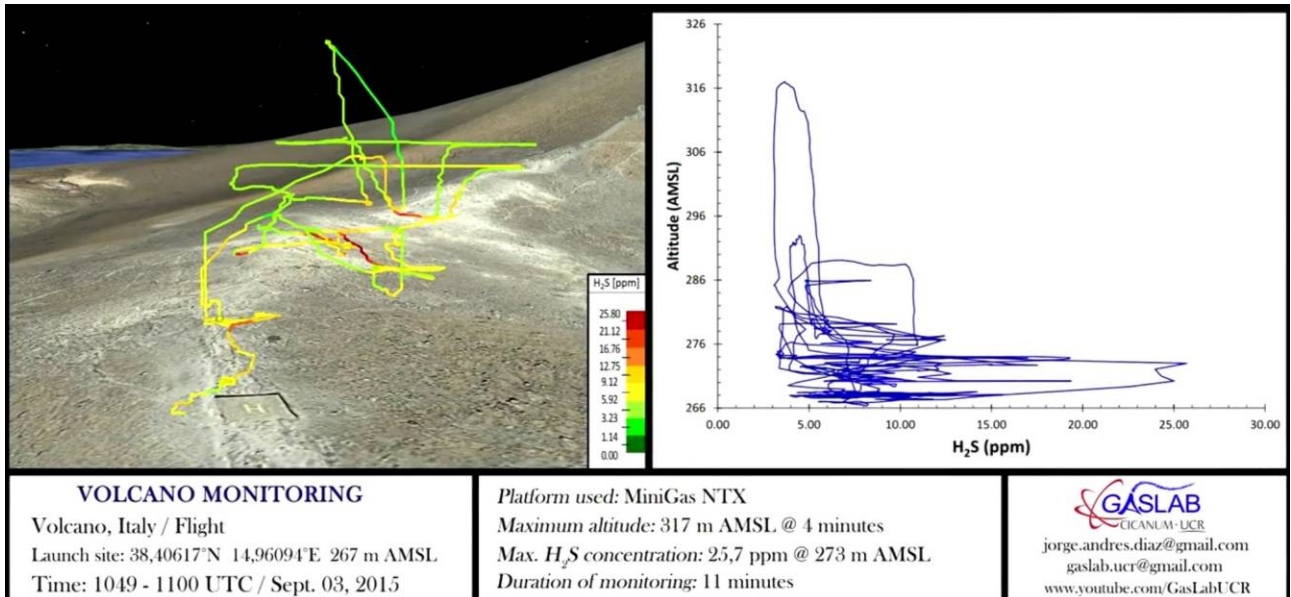


Figure 6. 3D view of H_2S concentration on Vulcano fumaroles crater. On the right picture: trend of the concentration of H_2S as a function of altitude. Trajectories in Google Earth™ images are colour-coded according to the legend on the left image. The measurements have been collected with the Italdrone Octocopter.

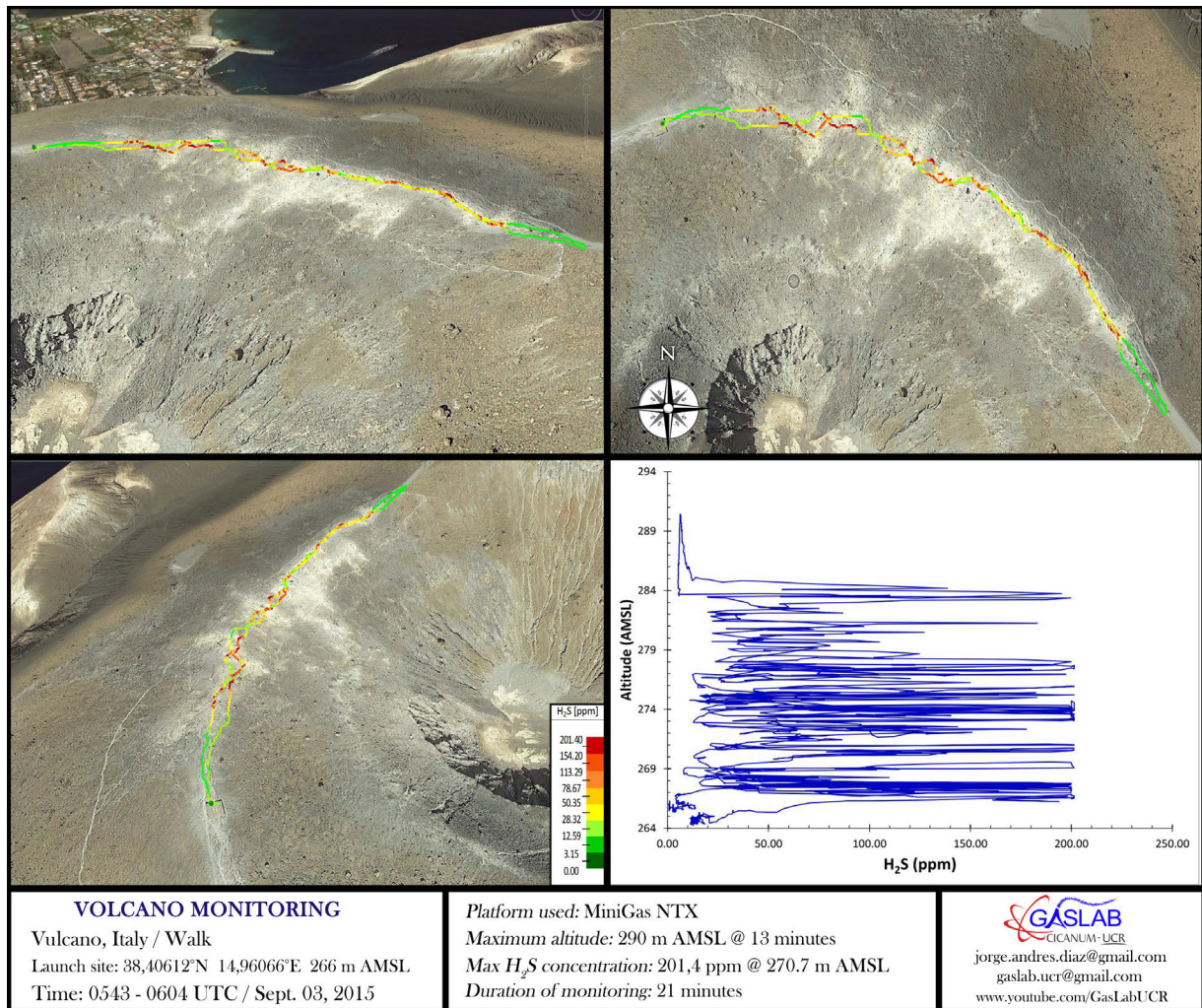


Figure 7. Ground Gas measurements. Pictures: 3D view of H_2S concentration on Vulcano crater fumaroles. Plot: trend of the concentration of H_2S as a function of altitude. Trajectories in Google Earth™ images are colour-coded according to the legend on the left image. The measurements have been collected had carrying the miniGAS along the rim of the Vulcano Crater.

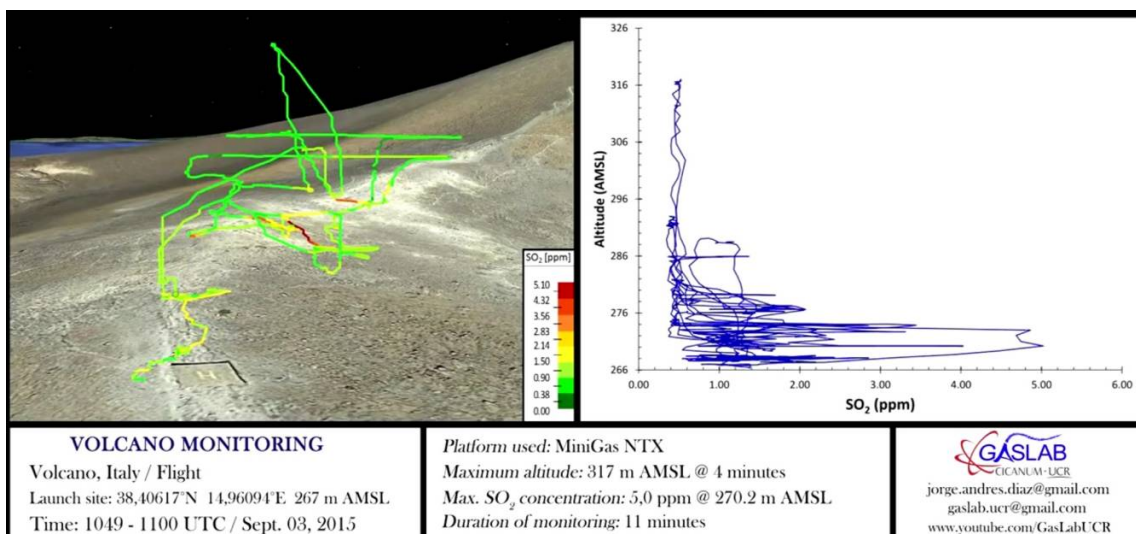


Figure 8. Left picture: 3D view of SO_2 concentration on Vulcano crater fumaroles. Right picture: trend of the concentration of SO_2 as a function of altitude. Trajectories in Google Earth™ images are colour-coded according to the legend on the left. The measurements have been collected with the Italdrone Octocopter.

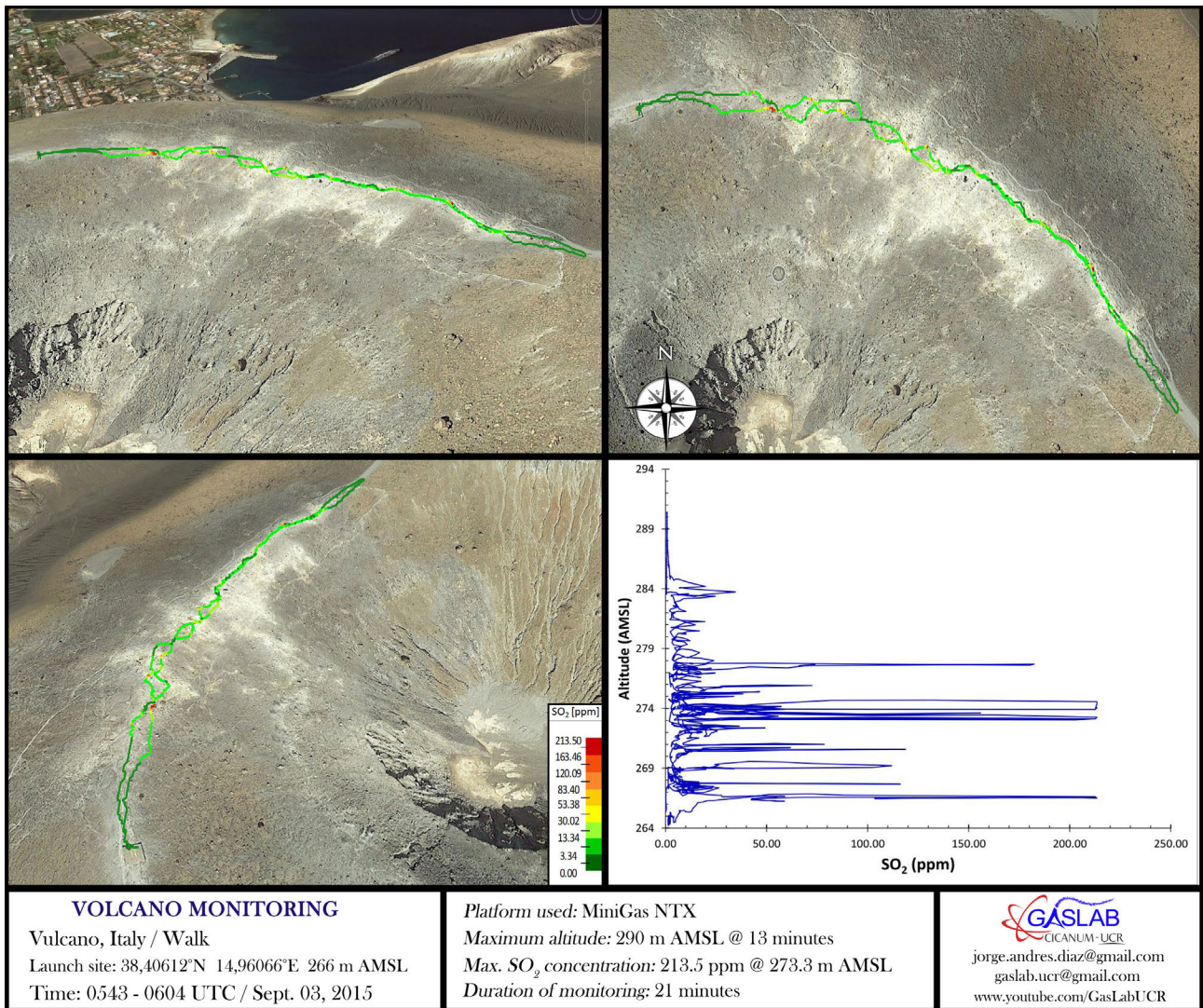


Figure 9. Ground Gas measurements Pictures: 3D view of SO₂ concentration on Vulcano crater fumaroles. Plot: trend of the concentration of SO₂ as a function of altitude. Trajectories in Google Earth™ images are colour-coded according to the legend on the left picture.

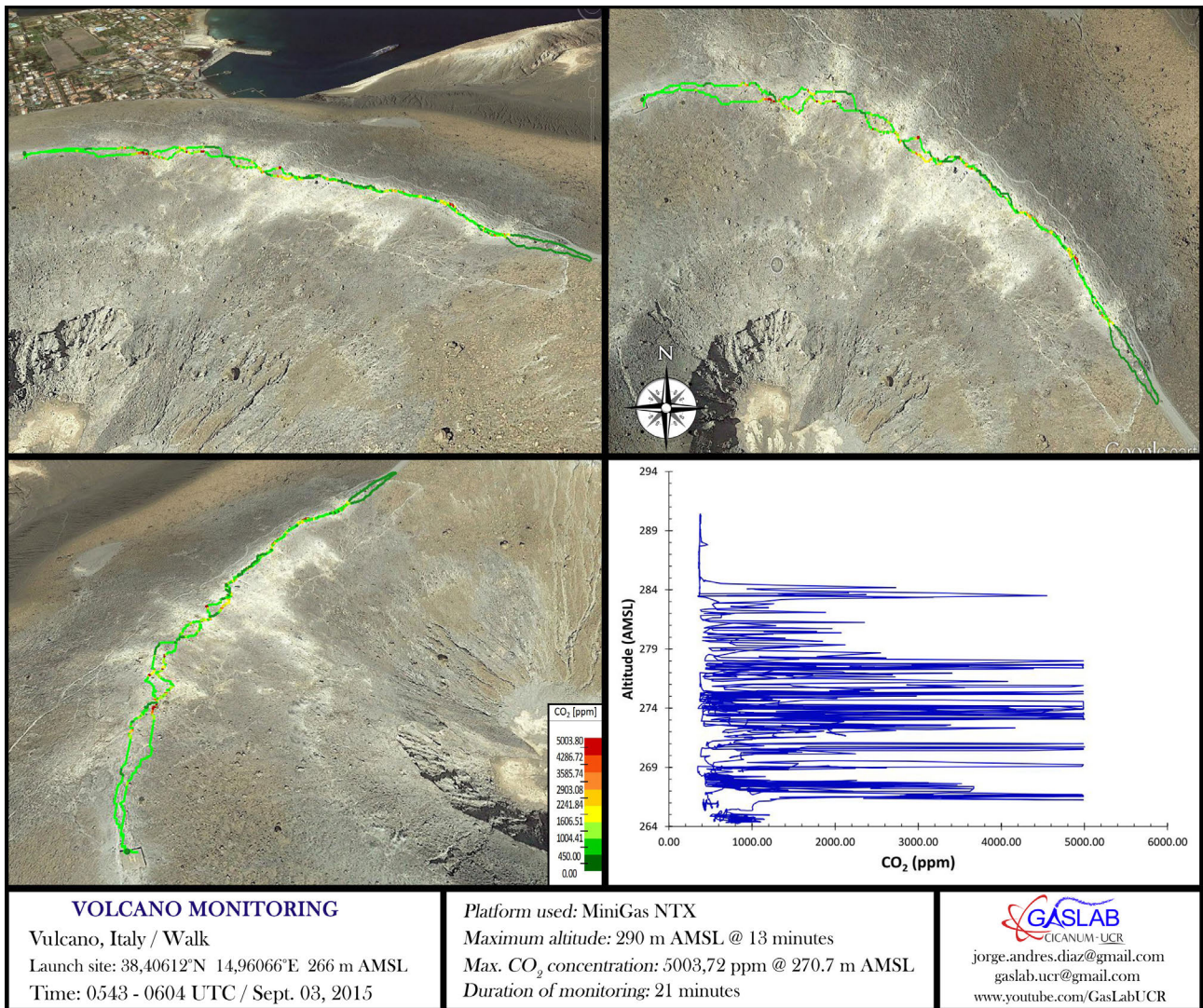


Figure 10. Ground Gas measurements Pictures: 3D view of CO₂ concentration on Vulcano crater fumaroles. Plot: the trend of the concentration of CO₂ as a function of altitude. Trajectories in Google Earth™ images are colour-coded according to the legend on the left picture. The measurements were collected hand-carrying the miniGAS along the rim of the Vulcano Crater.

In Figure 11 and Figure 12 the Vulcano plume characterization acquired using the MiniGAS instrument versus time and altitude are reported.

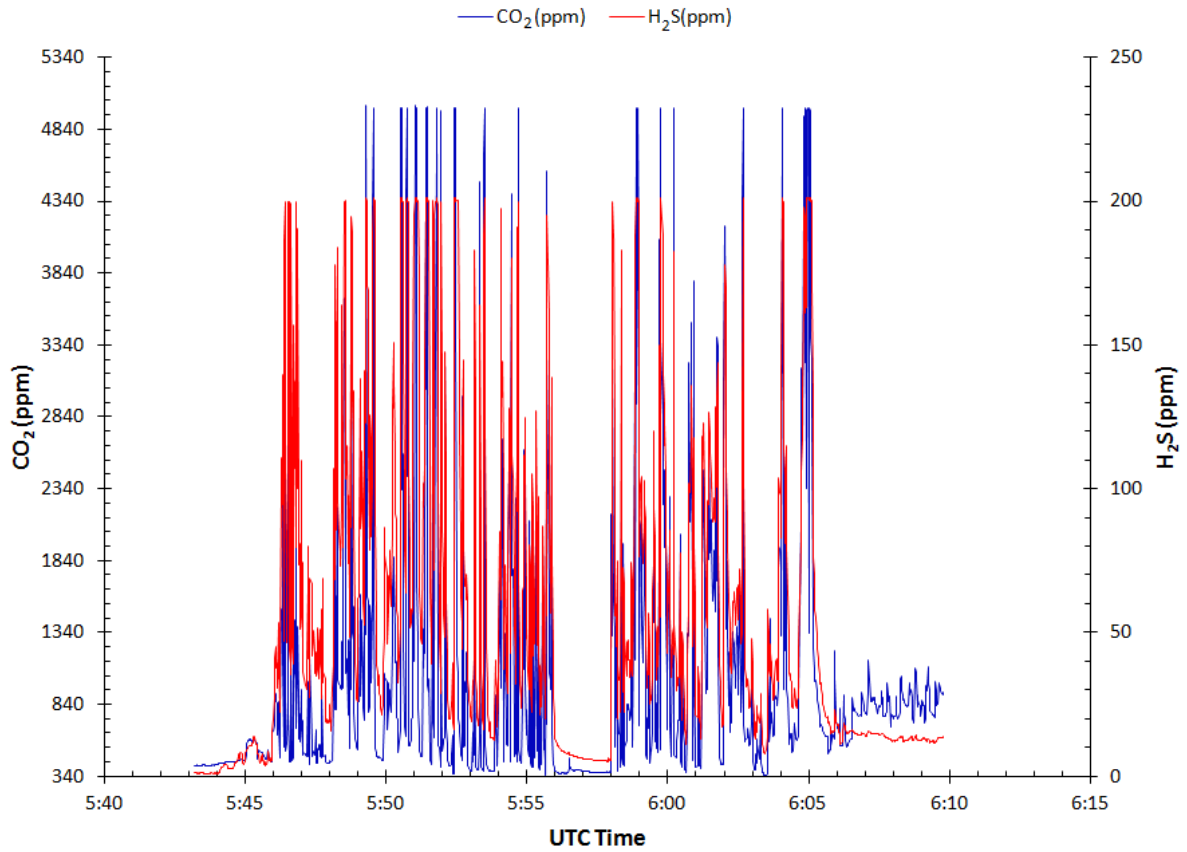


Figure 11. Vulcano plume characterization vs time using MiniGAS instrument: CO₂ and H₂S concentrations vs time.

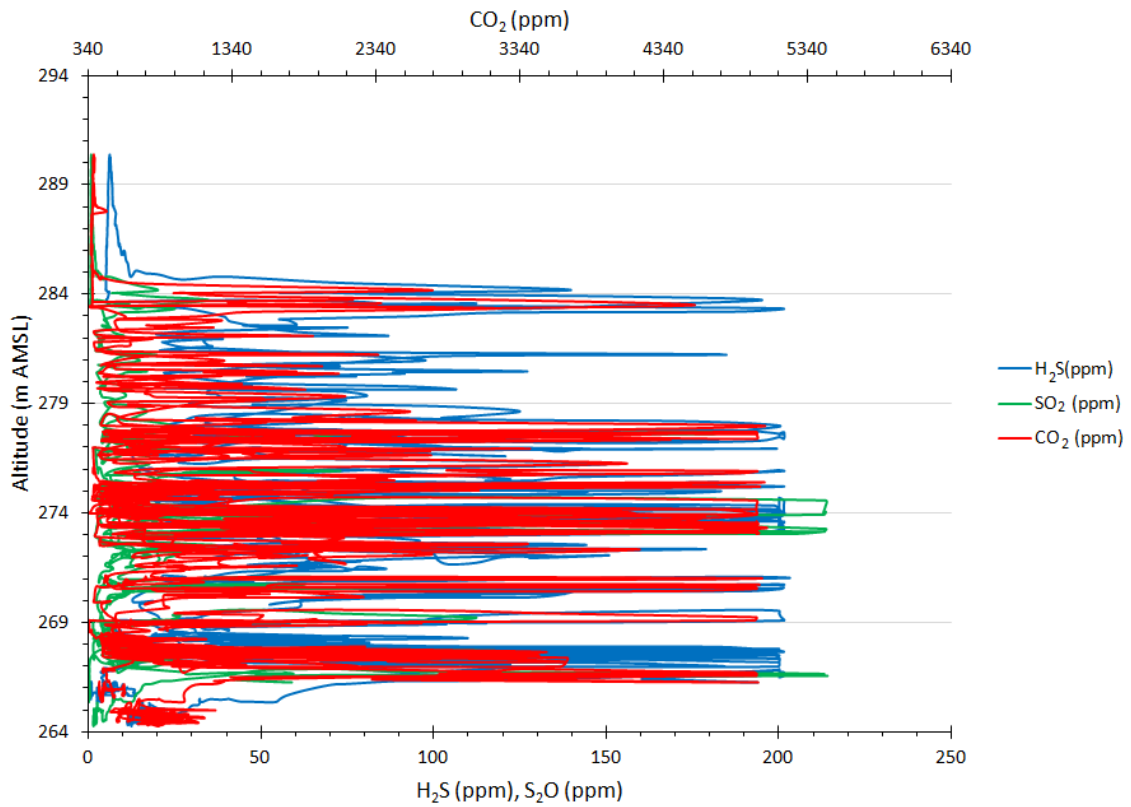


Figure 12. Vulcano plume characterization vs altitude using MiniGGAS instrument: SO₂, H₂S and CO₂ concentration vs Altitude.

2.1.3 Multigas analysis using Portable mass spectrometers (UAS-MS-MPH and UAS-MS-XPR3 Systems)

Two different mass spectrometers have been used during these campaigns. The first one was the UAS-MS XPR3, which is an upgraded version of the one previously used in the 2014 Solfatara campaign [Silvestri et al., 2015]. The UAS-MS-XPR3 tested at Solfatara is based on the Transpector XPR3 mass spectrometer from INFOCON, which is the latest generation of high-pressure, quadrupole-based process gas analysis mass spectrometer capable of operating in the mTorr (10^{-3} Torr) vacuum range; it is the smallest miniature commercial MS suited to volcanic gas analysis. The miniature ion source and quadrupole can operate from UHV to 20 mTorr and an especially designed electron multiplier (EM) will operate up to 10 mTorr. The XPR3 is well suited for portable MS when combined with the smallest turbo pump technology developed by CREARE LLC. It is 14.3 x 12.4 x 17.5 cm in dimensions and slightly over 1 kg. The Transpector XPR3 is controlled using INFOCON's FabGuard Suite of software loaded into a single board computer (Fit PC3) to acquire the MS and MiniGAS, data, store them and transmit them [Silvestri et al., 2015].

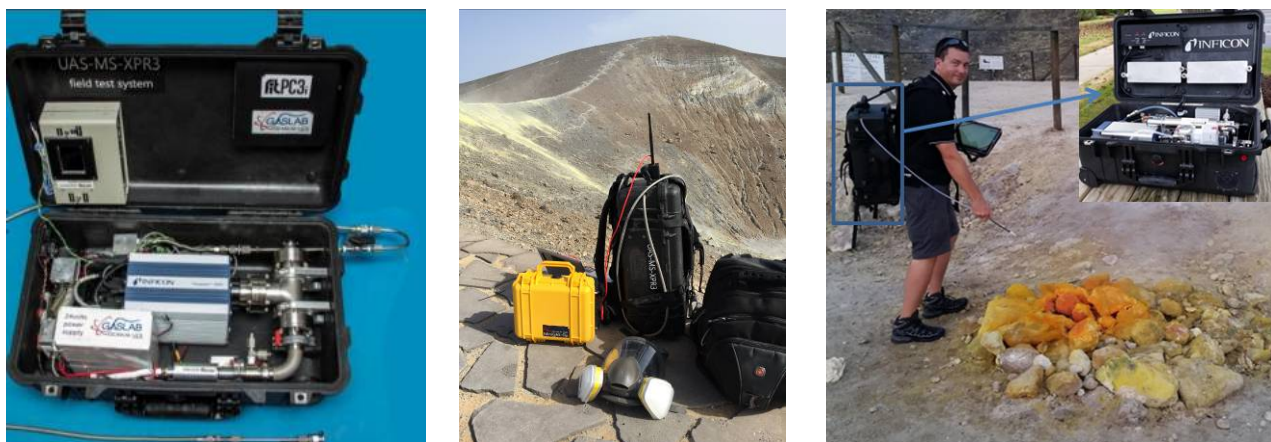


Figure 12. UAV-MS XPR3 Instrument (left and middle), UAS-MS MPH instrument (right).

The second MS tested was the UAS-MS MPH, designed for the *in situ* gas analysis using mid-size UAVs; it is based on the INFOCON Transpector MPH linear quadrupole MS, coupled with a Pfeiffer Vacuum HiPace10 Lite turbo pump with a direct inlet capillary. The Transpector MPH can measure in the range 0-200 m/z, has dual-coated filaments, an electron multiplier and built-in controller for turbo pump and gauge (it could also control inlet valves, although none was installed in this version). It has an onboard computer (Fitlet PC, 7 W) running Windows OS and the control software (FabGuard®). The used system requires < 60 W power and can be run for ≥ 4 hours using two batteries. The system is protected by a 1510 Pelican case (5.5 kg, carry-on size) and weighs approximately 19 kg.

The system performed well. The inlet was very fast (response time <300 ms) and showed little water carry over. The probe was not designed to be inserted directly into the fumarole, but future design will be ruggedized for such purpose. Methane was easily detected, but there were problems with H₂S and SO₂ detection. An initial issue was the exclusion of O₂ from the volcanic gas that caused the H₂S m/z channels to decrease because of the loss of O₂ isotopes (seen as lowering of H₂S signal - see Figure 14 data). A future version of FabGuard will be designed so as to compensate for oxygen depletion with real time data analysis. Secondly, the H₂S reacted with the stainless steel of the inlet system to produce SO₂. This can be seen in the Figure 14 data as a slow increase of the SO₂ signal. This can be avoided by using a fully coated inlet system. As seen in Figure 14, the SO₂ signal in the MS (m/z = 64 amu) has a different response time than the CH₄ signal (m/z = 16 amu) when exposed to the fumarolic gas; this difference has to do with the interaction of the SO₂ present in the sample with the stainless steel capillary used to introduce the gas to the MS, which, when going from low SO₂ to high SO₂, slowed the response time. The same chemical interaction also affected the recuperation time, the SO₂ slowly went down to normal levels after the few seconds of gas exposure as seen with the CH₄ signal. In a newer version of the MS system, a PEEK capillary is used to avoid this interaction and improve the response time.

The H₂S signal monitored at m/z = 34 goes down when exposed to the fumaroles gas due to the contribution of the oxygen isotope which also has m/z = 34 amu. When exposed to air, 34 was high especially due to the oxygen contribution, then when exposed to the fumaroles gas, oxygen went down, at a higher rate than the increase of H₂S, having a net effect of a decrease on the 34 amu signal. Figure 15 reports the time variation of the gases measured with UAS-MS MPH at the fumaroles of Vulcano summit crater.

Another version of this instrument includes a membrane inlet for trace detection (ppb or lower) of hydrocarbons. It is currently deployed in Chili/Antarctica for both direct MS and MIMS measurements.

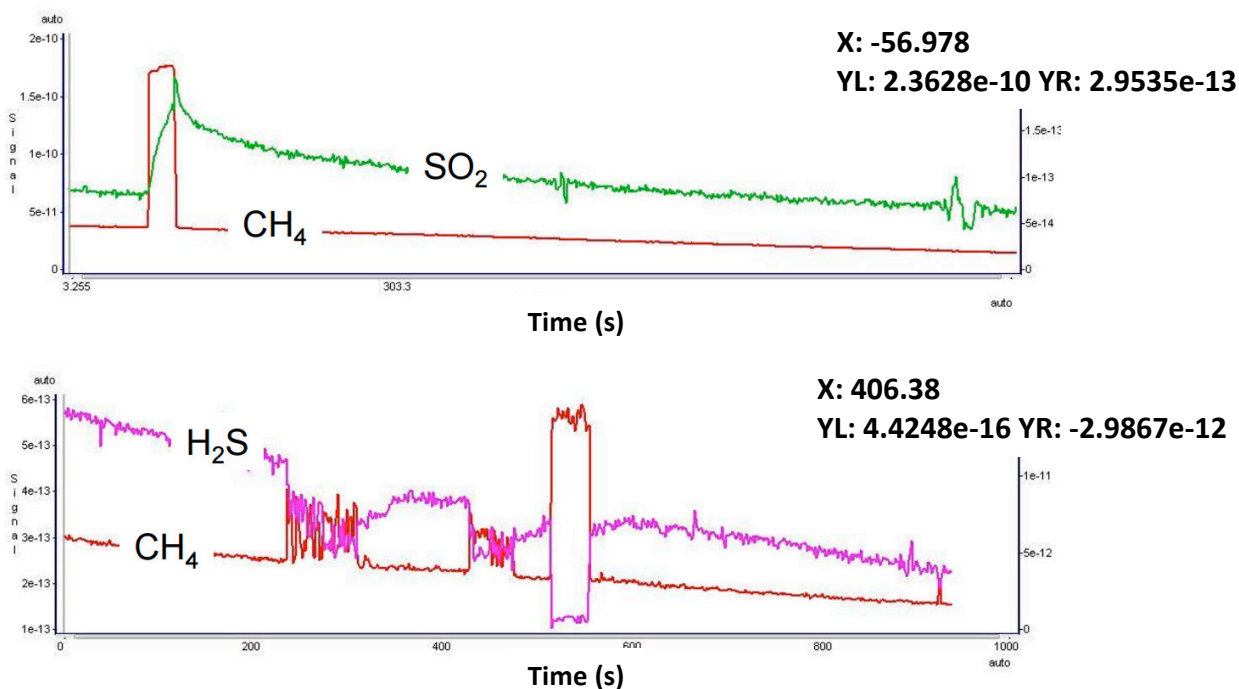


Figure 13. Time variation of gases collected at Solfatara fumaroles.

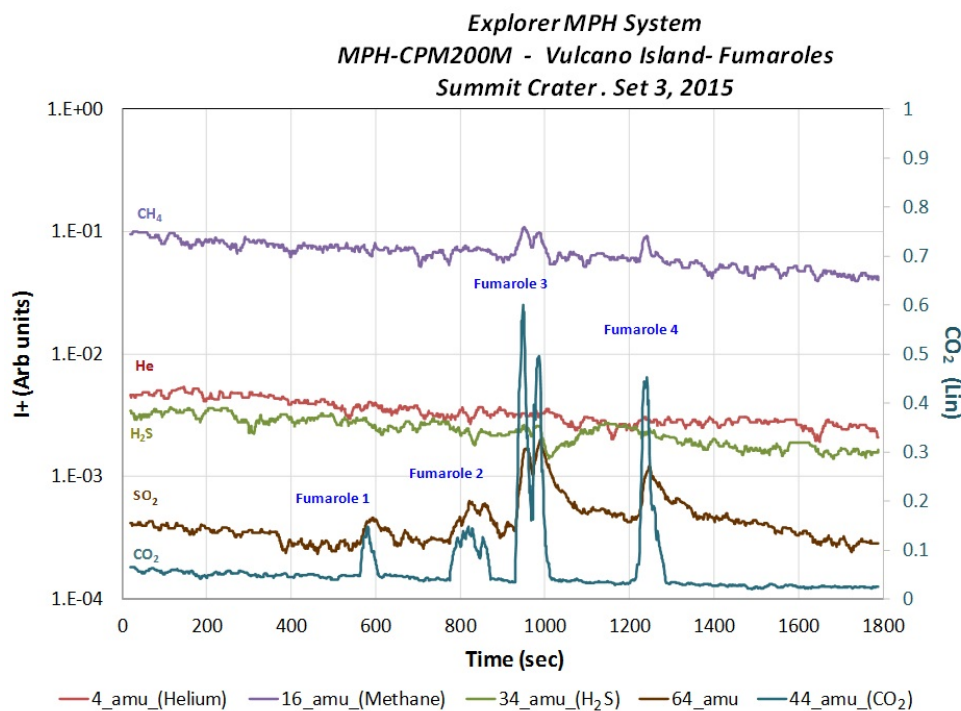


Figure 15. Time variation of the concentration of gases measured with UAS-MS MPH at fumaroles of Vulcano summit crater.

Measurements have been also performed in water (Figure 16) at Vulcano, near the area where underwater fumaroles are presents. The water temperature in this area is high (about 40-45°C) as also demonstrated by the measures recorded by the thermal camera (see 2.4, Figure 29). Temperature of the fumaroles was 100 °C (boiling water at sea level) and the out-gassing was measured with the UAS-MS-MPH instrument carried in backpack mode through the water. The gases present were CO₂ in large quantities, CH₄, H₂S in lower quantities and SO₂ in trace levels. These are typical magmatic gases in hydrothermal systems, but the measurements showed a small quantity of SO₂ not been scrubbed by the hydrothermal system. The SO₂ response time was much slower, which explain the lack of correlation between the H₂S, CO₂ and SO₂ signals.

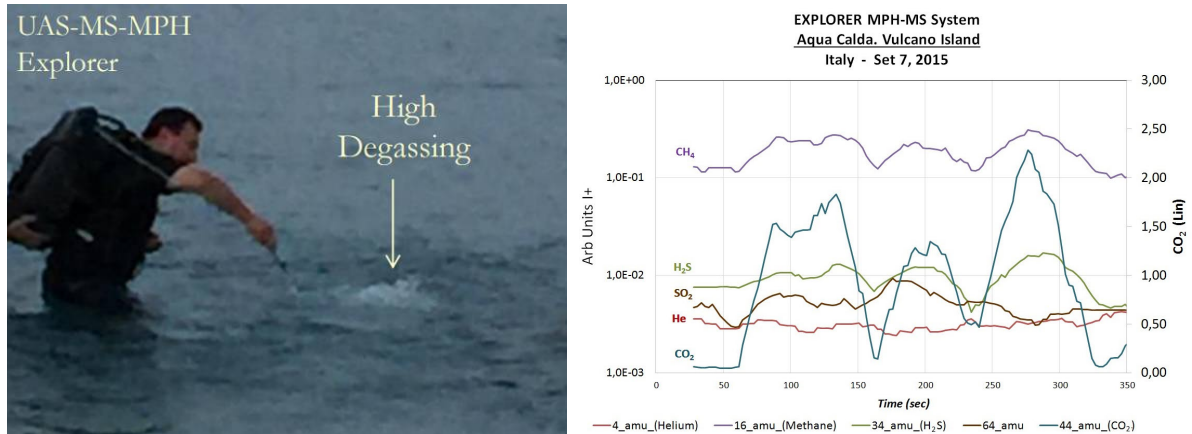


Figure 14. Gases measured with UAS-MS-MPH in water.

2.1.4 Drones and DEM test on Vulcano Crater

During the campaigns on Vulcano crater three different drones (Figure 17) were used, as shown in the table below:

Model	Max. Payload	Autonomy	Purpose
Quadcopter, DJI Phantom Vision plus 2	600 grams	6 min	Photogrammetry
Hexacopter DJI S800	950 grams	10 min.	Gas Sampling
Octocopter, ITALDRON E-EPIC 8HSEMAX	10 kg	25 min	Gas Sampling

The DJI Phantom Vision 2 Quadcopter has been already used in the 2014 Solfatara campaign and its features are reported in Silvestri et al., [2015]. This drone has been used during the campaigns in order to collect photos and videos, whereas the S800 DJI Hexacopter and the E-EPIC 8 Italdrone Octocopter have been used in the Solfatara and in the Vulcano campaigns. On these drones the NTX miniGAS instrument has been installed, offering the possibility to analyze gases and to produce real time 3D gas concentration maps. The measurements have been collected during flying over the fumaroles, allowing a safe acquisition of volcanic emissions data.



Figure 15. Drones used during the campaigns: DJI Phantom Vision 2 Quadcopter (left), DJI S800 Hexacopter (center), EPIC 8 Italdrone Octocopter (right).

One of the most versatile application of the use of pictures taken with a drone is the reconstruction of the geometry of the surface of the surveyed zone using photogrammetric techniques. As shown in Figure 18, a 3D model of Vulcano crater has been made using the PhantomVision Plus camera and a GoPro continuous shooting mode. The DSM has been generated by commercial photogrammetry software from PIX4D. Better solutions using appropriated cameras mounted on more capable and well stabilized drones will be systematically used in future campaigns, in order to produce surface as accurate as possible and high resolution DEMs. A good GPS campaign will provide a better Ground control point (GCP) collection. All these solutions will reduce the errors in estimating the surface models and elements (Centimetric) and increase the pixel resolution.

A high resolution 3D models and orthophotos from different periods are a good tool for detection of morphological and pattern changes.

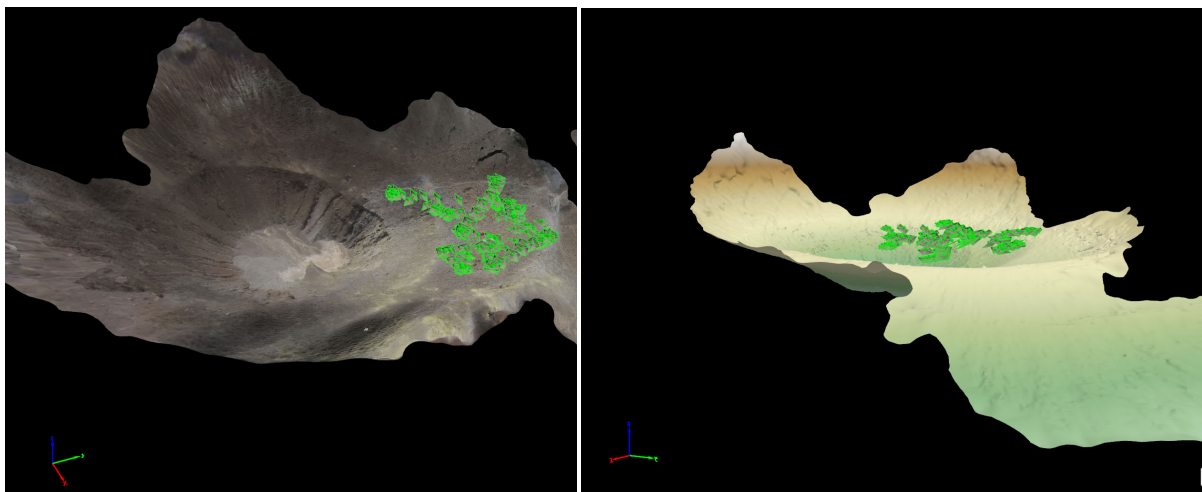


Figure 16. 3D model of Vulcano crater obtained using PhantomVision Plus camera planed mission and a GoPro continuous shooting mode.

2.2 SO₂ measurement using LP-Active DOAS and scanning DOAS

2.2.1 SO₂ measurements at la Solfatara and at Vulcano Island

On 1st and 3rd September 2015 SO₂ measurements were recorded, both at La Solfatara Volcano and at Vulcano Island by an active ultraviolet spectrometer system and by a two permanent passive scanning spectrometers instruments. The collected data were analysed applying the DOAS spectroscopy technique. LP-Active DOAS is a portable instrument and uses an artificial UV light source, while the Scanning DOAS, consists of a fixed instrument, performs real-time measurements in the volcanic plume, and uses the sun as a UV light.

LP-DOAS

The active long-path differential optical absorption spectroscopy (LP-DOAS) instrument, developed in fibre-coupling telescope technology and ultraviolet light emitting diodes (UV-LEDS), was designed to measure SO₂ gas and other trace gases such as, BrO, ClO, OClO, and NO₂ along well-defined open paths around volcanic vents [Vita et al., 2014; Kern et al., 2006] (Figure 19).

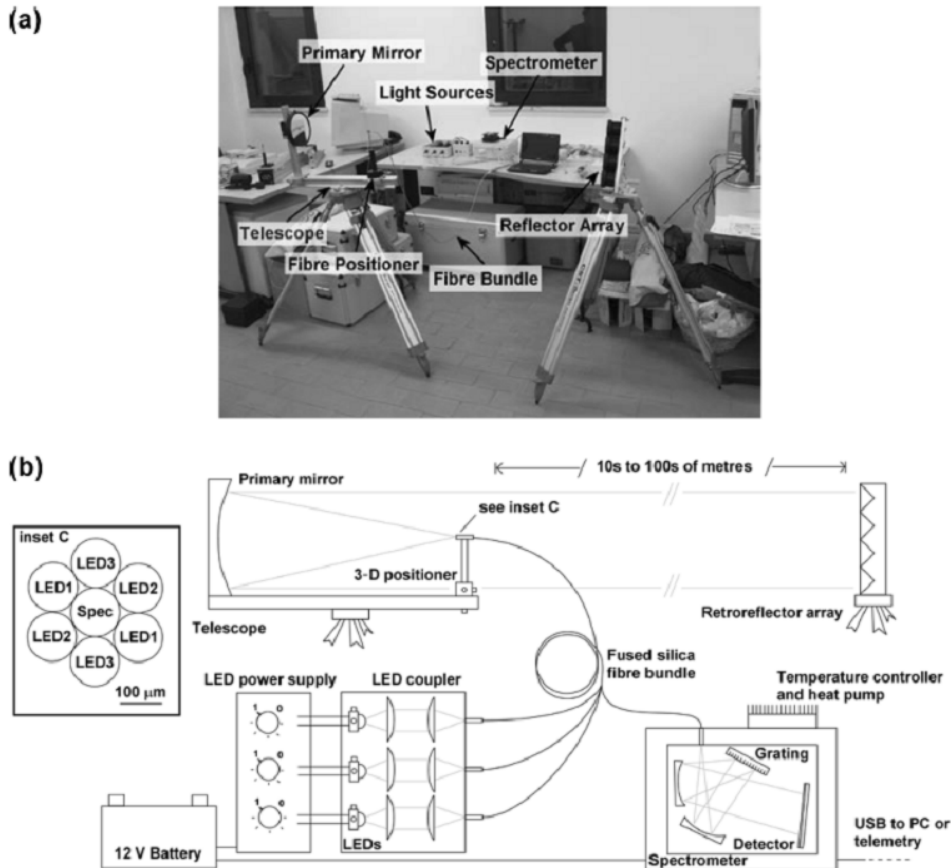


Figure 17. Photograph (a) and schematic model (b) of the portable active long-path DOAS instrument. Light from three UV LEDs is coupled to a fibre bundle, collimated to a parallel beam and sent to an array of reflectors. Upon returning, it is coupled to the spectrometer. The spectrum is analysed using an Ocean Optics QE65000 spectrometer with a cooled, back-illuminated CCD detector. The installed grating provided a wavelength range of 260 to 340 nm at a resolution of 0.5 nm.

2.2.2 Configuration of LP-DOAS measurements at La Solfatara Volcano

LP-DOAS measurements were performed at La Solfatara Volcano, on 01 September 2015, specifically at the fumaroles Bocca Nuova and Bocca Grande. The first set of measurements (between 13:42 h and 14:42 h) was carried out placing the retro-reflector at 9 meter away from the telescope, behind the fumarole of Bocca Nuova (Figure 20a).

The second set of measurements (15:09 h to 15:40 h) was carried out by placing the retro-reflector at 9 meter away from the telescope, behind the fumarole Bocca Grande (Figure 20b).

An array of retro-reflectors, composed by ten 52mm diameter fused silica corner cubes densely packed in a triangular frame with a total diameter of approximately 40 cm mounted on a tripod, was used to reflect the transmitted radiation through the sampling area, back to the telescope. The telescope component of the instrument is composed of an optical bench, in which are coaxially arranged the optical positioned fibre, which is used to mount the end of the fibre bundle in the focal plane of the mirror, and the primary mirror, which is equipped with micrometre heads for optic alignment. The fibre bundle consists of seven 100 µm diameter fused silica fibres, six of which are arranged in a circular pattern around a central seventh fibre. In this coaxial set-up, the telescope primary mirror acts both as a sending and receiving unit.

An Ocean Optics® QE65000 spectrometer with a spectral range between 260 and 345 nm was used to measure the spectrum of this incident radiation at intervals of a few seconds. The spectrometer was kept at a stable temperature of 20° using a Super Cool © PR-59 thermoelectric cooling/heating unit. The spectra were recorded on a small netbook computer. A 12 V battery was used to power the entire setup (see Vita et al., [2014], for more technical details).

Considering the very low abundance of SO₂ in the fluids emitted by the Solfatara fumaroles area (maximum value of 0.6 ppm at fumarole Bocca Grande on the October 2012 survey [Aiuppa et al., 2013]), about 2×10^{16} molec/cm² or about 8 ppm m which was actually below to the instrument's detection limit we could not evaluate the presence of SO₂ species and their relative amount in the analyzed gases. In future campaigns, we plan to repeat the field measurements with a different optical setup, enhancing the UV source in the strongest differential absorption lines of this chemical species.



Figure 20. Location of the LP-DOAS during the measurement period at La Solfatara on September 01, 2015. The reflectors are placed directly behind a higher temperature fumaroles a) Bocca Nuova, b) Bocca Grande.

2.2.3 Configuration of LP-DOAS measurements at Vulcano Island

LP-DOAS measurement were performed at La Fossa crater (Vulcano Island), on 03 September 2015, specifically at F0 fumaroles. Measurements were carried out from 09:44 h to 11:00 h local time. The array of retroreflectors was positioned on the rim of La Fossa crater, behind a high-temperature fumarole (F0) and about 9 m away from the telescope which corresponds to the width of the area affected by the fumarole emission (see Figure 21).



Figure 21. Photograph of the positioning of the Active-LP DOAS during the measurements made at Vulcano Island through the high temperature fumarole (F0).

During this time, the gases being emitted by this fumarole were measured along the optical path between reflector and UV-source. No disturbance from other fumaroles is expected in this data set, as favourable winds were blowing other fumaroles gases in the area away from the light path. Depending on the wind, the light path length through the fumarolic gases was between 0 and 9m one way, so the total light path resulted between 0 and 18m, which was enough to derive reasonable SO₂ column densities. The maximum detected SO₂ column was about $3e^{17}$ molec/cm² (Figure 22), which corresponds to about 120 ppm*m.

During the measurements the fumarolic gases pollution varied considerably inside the light path length due to variations in wind direction as well as variations in the intensity of the degassing strength of the fumaroles themselves.

The fluctuation is mainly caused by winds blowing the fumarolic gas into or out of the light path. The maximum values correspond to an average SO₂ mixing ratio of about 6.7 ppm in the fumarolic gas along the light path (assuming a light path length of 18 m for these measurements).

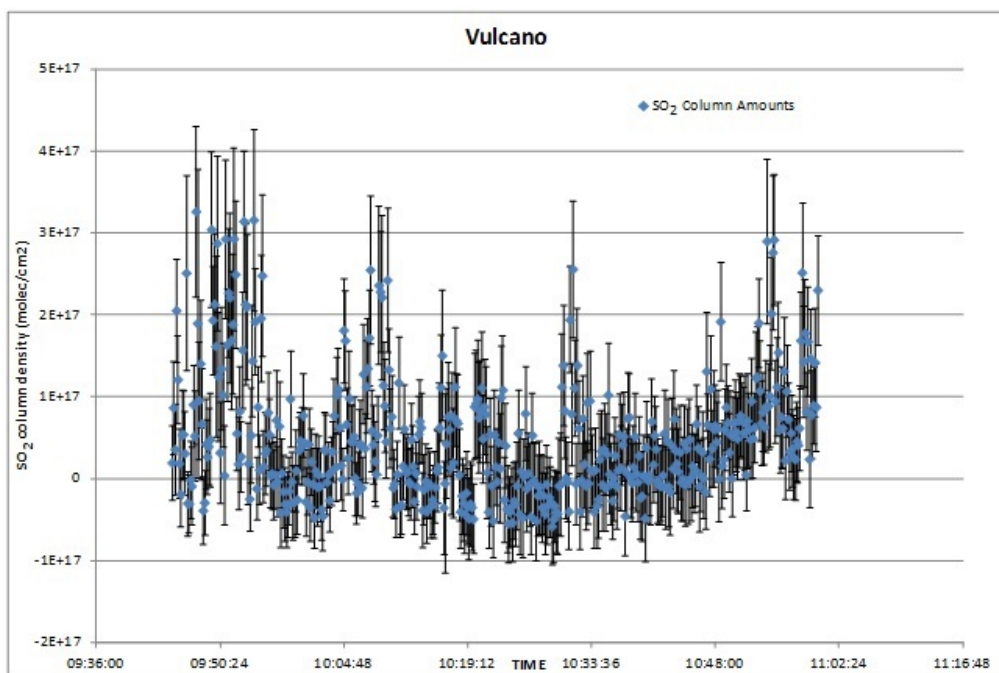


Figure 18. Time series of SO₂ (with error bar of each SO₂ measurements) recorded during the measurements on September 03, 2015. The SO₂ column density fluctuated between 0 and $3e^{17}$ molec/cm².

2.2.4 Configuration of Scanning DOAS measurements at Vulcano Island

UV Scanning DOAS Network

In the framework of the “Network for Observation of Volcanic and Atmospheric Change” (NOVAC), a worldwide network of permanent scanning DOAS instruments [Galle et al., 2010] was installed on 19 volcanoes around the world, to measure real-time volcanic SO₂ emission fluxes. Within this context, two fixed UV scanning DOAS instruments (see Vita et al., [2012], for more technical details) (Figure 23) were installed at Palizzi (the west side of Vulcano Island, near the active crater) (Figure 24d) in March 2008 and at Porto di Levante area in 2015 (Figure 24b), together with a weather station, on Lentia Hill (Figure 24c) at the same altitude (350 m a.s.l.) as La Fossa crater. The weather station provided information about wind speed and direction, rainfall, temperature, relative humidity, whereas the UV station provided, visible and infrared UV radiation. Through a wireless communication system (Figure 24a) the acquired data were then transmitted, in real-time via the internet, to the Vulcano Observatory and from there to the Istituto Nazionale di Geofisica e Vulcanologia (National Institute of Geophysics and Volcanology, INGV, Palermo).

The collected spectra were analyzed according to the DOAS procedures, which are based on the Beer Lambert’s Law. Each spectrum was first corrected for the electronic noise (offset and dark current). The optical density was obtained by dividing each spectrum measurement by a reference spectrum, such as a spectrum taken outside the plume, and the result of this calculated transmittance was converted into log₁₀ values [Platt and Stutz, 2008]. A polynomial of 5th order fitting to the acquired data was used to take into account any broadband extinction structures that were caused by broadband absorption of trace gases [Platt and Perner, 1983; Platt, 1994; Platt and Stutz, 2008]. A high-pass filter was applied to the absorption cross-sections in order to use only the remaining high frequency structure, which is unique for any trace gas, and which can therefore be used to determine its abundance. Shift and squeeze were allowed for the absorption cross-sections (SO₂ and O₃, Bogumil et al., [2003]), to compensate for any small shifts, caused mainly by the variations in the temperatures of the spectrometer and of the detector unit [Vita et al., 2012].

Values of SO₂ flux were averaged daily using all measurements taken during each day. The daily values of SO₂ flux ranged from 19 to 28 Tons/day, the highest value (28.1 ± 8.4 Tons/day) was recorded on September 7, while the lowest value (19.4 ± 6.5 tons/day) was recorded on September 5. On 3 and 4 September were recorded daily average values of SO₂ flux respectively of 25.2 ± 4.9 and 27.5 ± 6.3 tons/day (Figure 25).

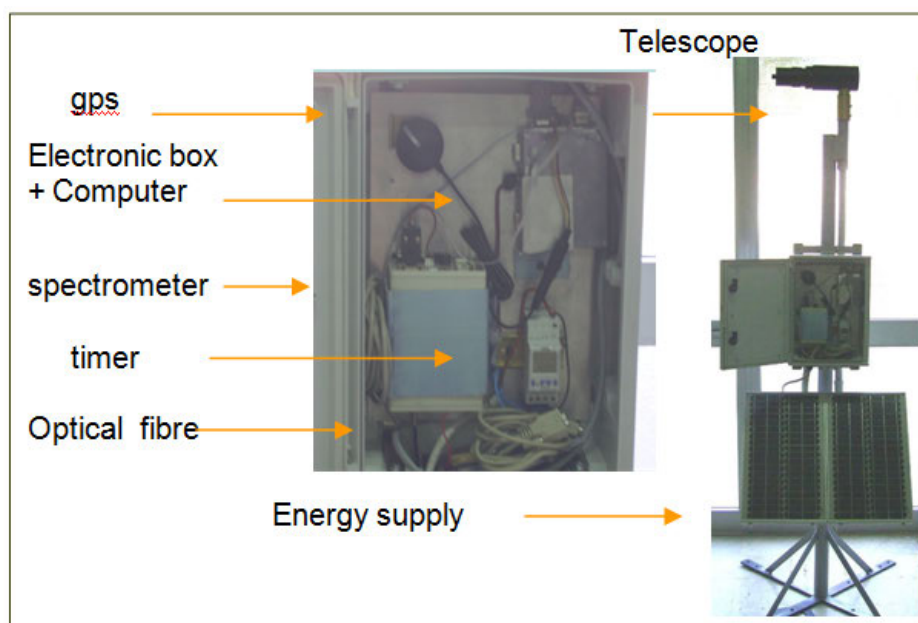


Figure 19. Photograph of the UV Scanning-DOAS system comprises a single spectrometer from Ocean Optics Company, an embedded PC, GPS receiver, optical fibre, and telescope.

Real Time SO₂ gas Monitoring Network at Vulcano Island

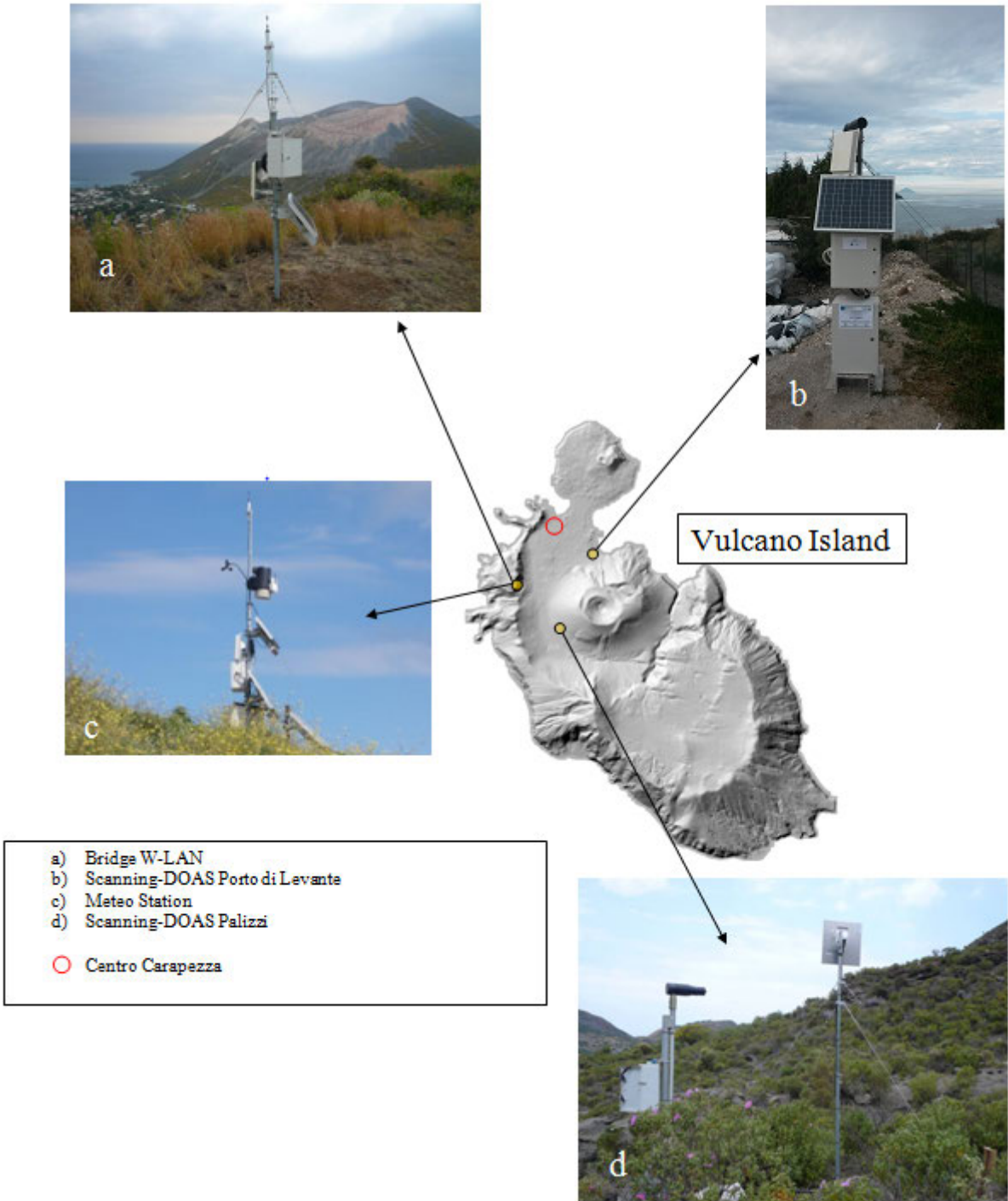


Figure 20. SO₂ Vulcano Network.

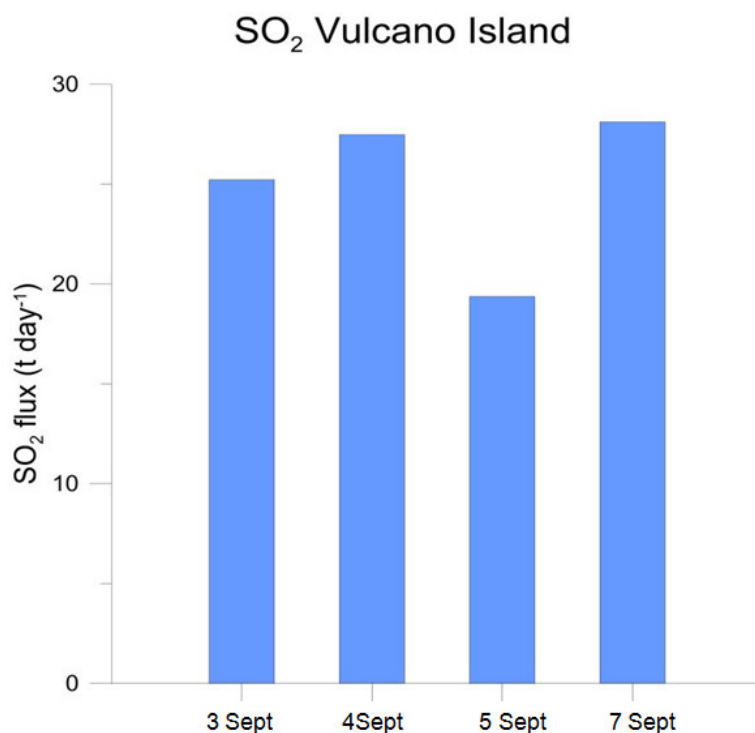


Figure 21. Time variation of the total flux of SO₂ emitted between 3 to 7 September 2015 at Vulcano Island; each value corresponds to the daily average of the measurements taken from the network of Scanning DOAS installed permanently on the island.

2.3 Photometric Measurement

During the Vulcano field campaign, in order to characterize the atmospheric particulate, measurements of aerosol optical thickness (AOT) have been collected on two different sites: Vulcano crater and “Pozza dei fanghi”. The measurements have been performed using a portable MICROTOPS II model Solar Light sun-photometric. This instrument is a Volztype photometer with a 2.5° field of view and is owned by remote sensing laboratory belonging to the “Satellite data for Earth Observation” INGV-CNT Unit. Thanks to its reduced size it is largely used in field campaigns in various remote areas as volcanic areas [Colini et al., 2014, Porter et al., 2002 and Watson and Oppenheimer, 2001] or desert areas [Musacchio et al., 2015].

Information on the main features of this instrument can be found on the website of the NERC Field Spectroscopy Facility [<http://fsf.nerc.ac.uk/instruments/sunphotometer.shtml>].

The sun-photometer was operated during the field campaign and performed direct solar irradiance measurements at 5 different wavelengths from UV to near IR (440, 675, 870, 936 and 1020 nm), providing AOT at each wavelength from the surface up the Sun looking toward the atmosphere [Holben et al., 2001], along with the water vapor column content at different wavelengths. Other information concerning the optical and microphysical aerosol properties (such as the refractive index and the aerosol size distribution), which are necessary for the atmospheric characterization in the surface spectral retrieving process, are systematically retrieved from the sun-photometer measurements. A proper use of this instrument requires that its fore-optic points toward the solar disk and for such a reason the instrument, for human eye safety, has an indirect tracking system that can be easily handled by mounting the sun-photometer on a tripod. Figure 26 shows the instrument set up and Figure 27 reports the measurements of the aerosol optical thickness collected in 5 different wavelengths (original data are shown in Table 1).



Figure 22. Microtops sun photometer mounted on its tripod with connected GPS.

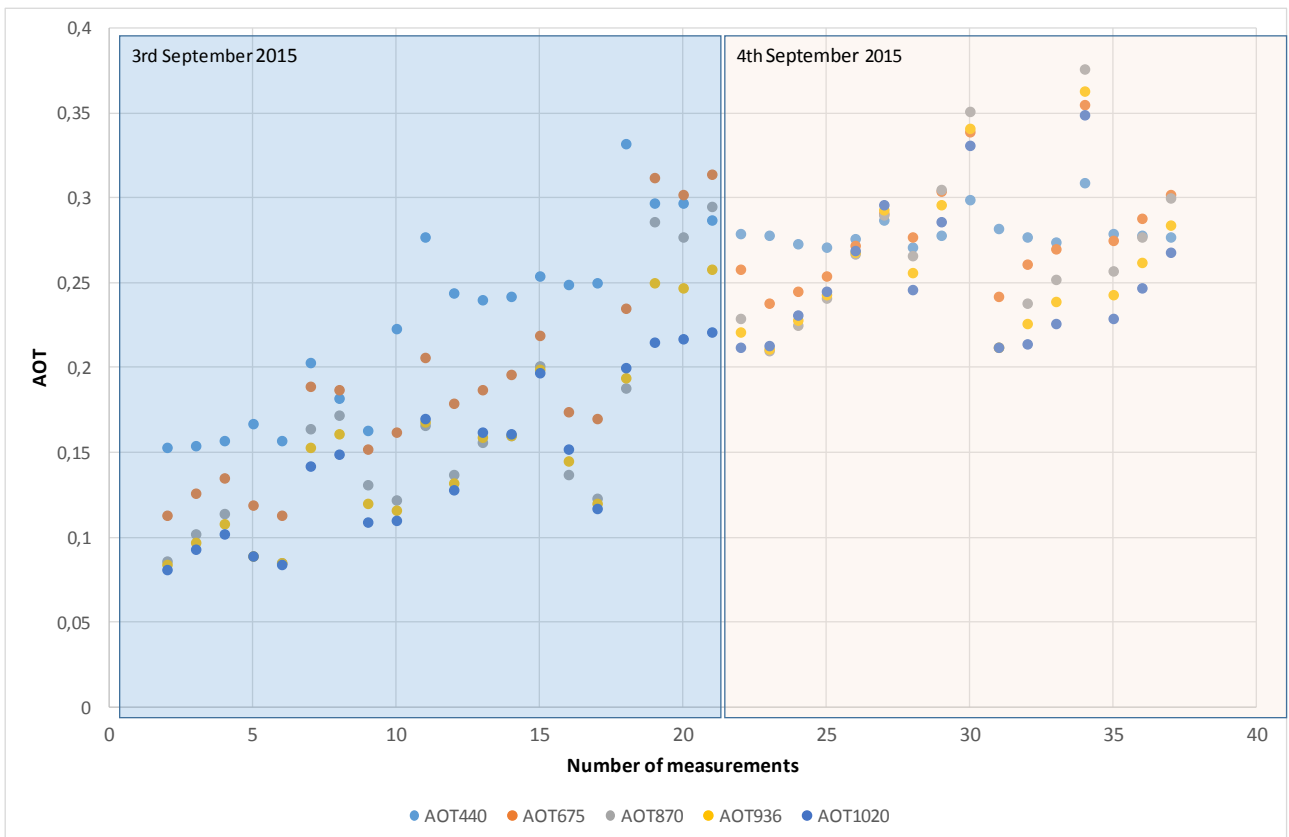


Figure 23. Photometric Measurement. Total aerosol optical thickness (AOT) trend obtained by sampling the atmosphere by using Microtops sun photometer. The optical thickness is represented as a function of the wavelength measurements acquired during the field campaign.

N° Meas.	DATE	TIME	LATITUDE	LONGITUDE	SAZ	AOT440	AOT675	AOT870	AOT936	AOT1020
1	03/09/2015	05:21:10	38,406	14,961	81,06	1,043	1,068	1,066	1,064	1,061
2	03/09/2015	05:41:09	38,406	14,961	77,14	0,153	0,113	0,086	0,084	0,081
3	03/09/2015	05:41:51	38,406	14,961	77,01	0,154	0,126	0,102	0,097	0,093
4	03/09/2015	05:42:10	38,406	14,961	76,95	0,157	0,135	0,114	0,108	0,102
5	03/09/2015	05:45:06	38,406	14,961	76,37	0,167	0,119	0,089	0,089	0,089
6	03/09/2015	05:45:27	38,406	14,961	76,3	0,157	0,113	0,085	0,085	0,084
7	03/09/2015	06:42:21	38,406	14,961	65,23	0,203	0,189	0,164	0,153	0,142
8	03/09/2015	06:43:07	38,406	14,961	65,08	0,182	0,187	0,172	0,161	0,149
9	03/09/2015	06:43:27	38,406	14,961	65,01	0,163	0,152	0,131	0,12	0,109
10	03/09/2015	08:04:30	38,406	14,961	49,98	0,223	0,162	0,122	0,116	0,11
11	03/09/2015	08:04:51	36,067	14,961	48,91	0,277	0,206	0,166	0,168	0,17
12	03/09/2015	08:05:13	38,406	14,961	49,86	0,244	0,179	0,137	0,132	0,128
13	03/09/2015	08:05:30	38,406	14,961	49,81	0,24	0,187	0,156	0,159	0,162
14	03/09/2015	08:05:50	38,406	14,961	49,75	0,242	0,196	0,16	0,16	0,161
15	03/09/2015	08:06:06	38,406	14,961	49,7	0,254	0,219	0,201	0,199	0,197
16	03/09/2015	08:13:54	38,406	14,961	48,35	0,249	0,174	0,137	0,145	0,152
17	03/09/2015	08:14:16	38,406	14,961	48,29	0,25	0,17	0,123	0,12	0,117
18	03/09/2015	10:28:53	38,406	14,961	31,59	0,332	0,235	0,188	0,194	0,2
19	03/09/2015	10:29:22	38,406	14,961	31,57	0,297	0,312	0,286	0,25	0,215
20	03/09/2015	10:29:39	38,406	14,961	31,55	0,297	0,302	0,277	0,247	0,217
21	03/09/2015	10:29:56	38,406	14,961	31,54	0,287	0,314	0,295	0,258	0,221
22	04/09/2015	08:01:31	38,416	14,96	50,71	0,279	0,258	0,229	0,221	0,212
23	04/09/2015	08:02:16	38,416	14,96	50,58	0,278	0,238	0,21	0,211	0,213
24	04/09/2015	08:02:41	38,416	14,96	50,51	0,273	0,245	0,225	0,228	0,231
25	04/09/2015	08:02:58	38,416	14,96	50,46	0,271	0,254	0,241	0,243	0,245
26	04/09/2015	08:03:15	38,416	14,96	50,41	0,276	0,272	0,267	0,268	0,269
27	04/09/2015	08:03:29	38,416	14,96	50,37	0,287	0,291	0,29	0,293	0,296
28	04/09/2015	08:03:53	38,416	14,96	50,3	0,271	0,277	0,266	0,256	0,246
29	04/09/2015	08:04:08	38,416	14,959	50,25	0,278	0,304	0,305	0,296	0,286
30	04/09/2015	08:04:23	38,416	14,959	50,21	0,299	0,339	0,351	0,341	0,331
31	04/09/2015	08:45:50	38,416	14,96	43,33	0,282	0,242	0,212	0,212	0,212
32	04/09/2015	08:46:30	38,416	14,96	43,22	0,277	0,261	0,238	0,226	0,214
33	04/09/2015	08:46:46	38,416	14,96	43,18	0,274	0,27	0,252	0,239	0,226
34	04/09/2015	09:33:39	38,416	14,96	36,69	0,309	0,355	0,376	0,363	0,349
35	04/09/2015	09:33:59	38,416	14,96	36,65	0,279	0,275	0,257	0,243	0,229
36	04/09/2015	09:34:14	38,416	14,96	36,62	0,278	0,288	0,277	0,262	0,247
37	04/09/2015	09:34:36	38,416	14,96	36,58	0,277	0,302	0,3	0,284	0,268

Table 1. Measurements of Aerosol Optical Thickness in the five different wavelengths, with Sun Zenit Angle (SAZ) information.

2.4 Thermal measurements

Measurements on surface temperature have been collected with Thermotecnix VISIR640 of optical lab UF-8 (INGV-CNT). The Thermotecnix VISIR640 is a highly sensitive thermal camera (640 x 480 pixels) with spectral range from 7.5 to 13 μm , accuracy of ± 2 $^{\circ}\text{C}$ (or $\pm 2\%$ of reading) and 60 mk thermal sensitivity. The main sites where the thermal information was collected were for fumaroles of Bocca Nuova

and Bocca Grande at the Solfatara (Figure 28) and the crater of “La Fossa”, where main fumaroles are present, and the “Pozza dei fanghi” area at Vulcano island (Figure 29). The measurements were acquired both during the daytime and at nighttime.

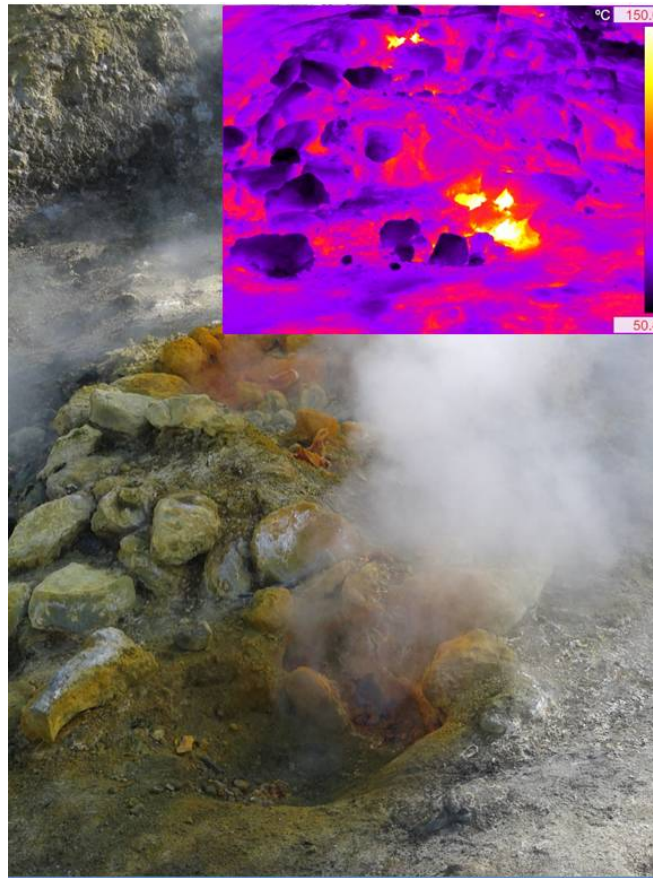


Figure 24. The “Bocca Grande” fumarole and Infrared Images acquired with Thermotecnix VISIR640 Thermo-camera.

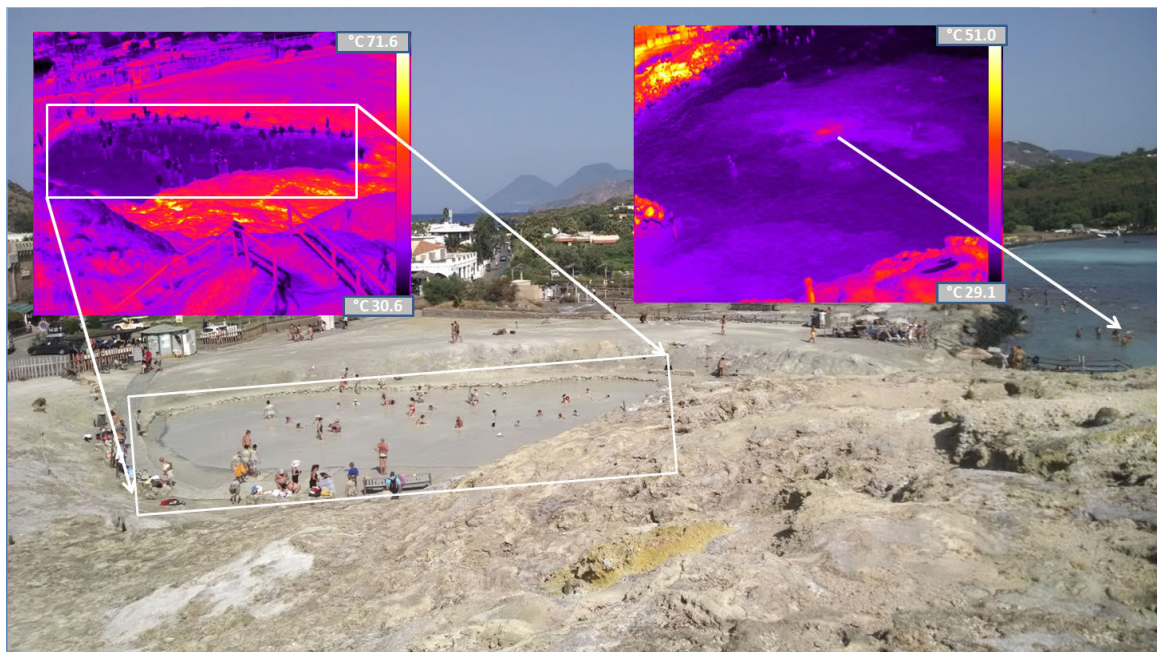


Figure 25. The “Pozza dei fanghi” and the relevant Infrared Images there acquired with the Thermotecnix VISIR640 Thermo-camera.

A night-time measurement was carried out at Vulcano Island on 4th September, at a site located at the SW foot of the La Fossa cone (Figure 30). This site is characterized by strong diffuse gases emission and the presence of a hot spot.

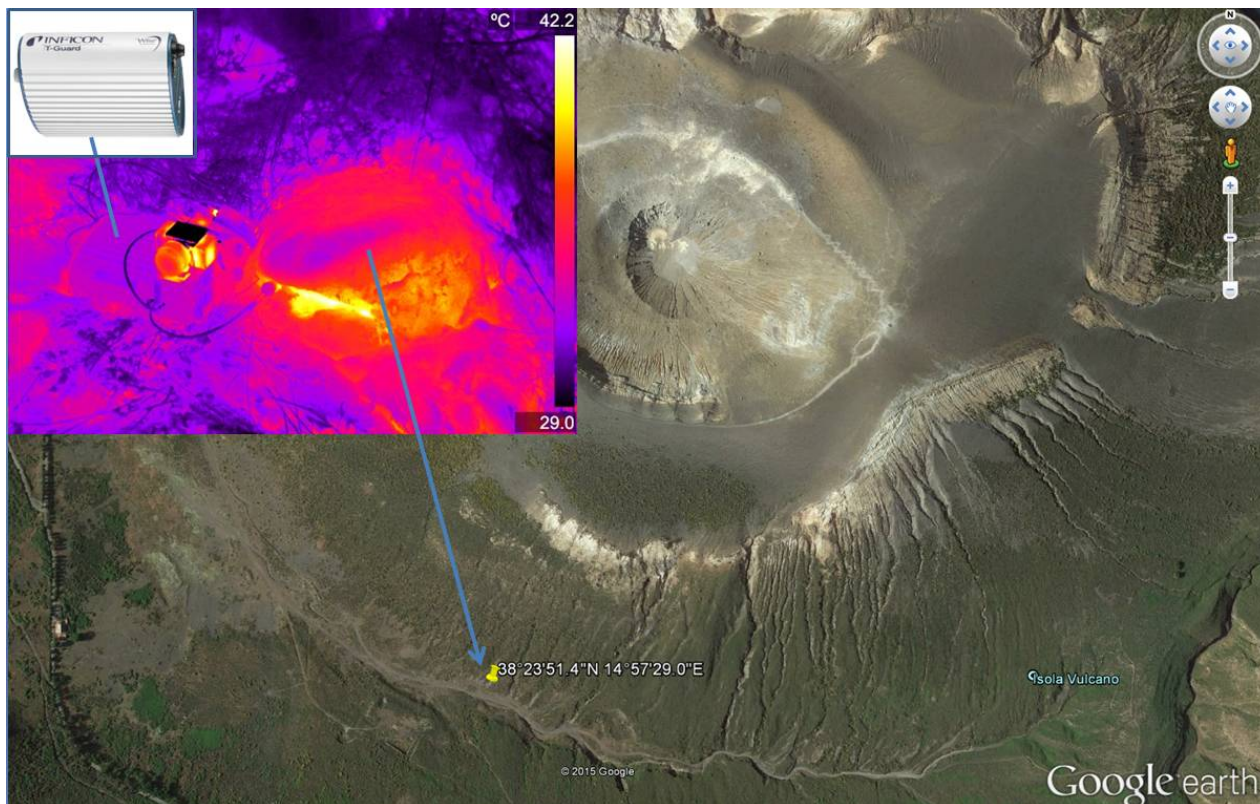


Figure 30. Hot spot highlighted with the Thermotecnix VISIR640 Thermo-camera during helium measurements performed with the T-Guard instrument.

2.5 Radiance and reflectance measures

Measurements of radiances and reflectance on Vulcano Island using the ASD Field Spec Pro spectrometer were performed during the campaign of September 3rd. This instrument is a portable spectrometer with optical fiber used for field campaign and laboratory. It operates in the spectral range 250-2500 nm with a spectral resolution of up to 3 nm. The measurements were made at different sites on the island (on the volcano crater, on the “Pozza dei Fanghi”, on the black sand beach of Porto di Ponente and Porto di Levante harbour), whose positions were detected by GPS and with good weather conditions (clear sky). The reflectance spectra were acquired at a height of 70cm above the ground. These *in situ* measurements provided a useful ground comparison and validation for satellite data

Reflectances were measured considering both the data from past field campaigns and new data from new sites (Figure 31 - Figure 34 and Table 2). For each site 30 reflectance spectra were acquired and then the mean values were computed.

This kind of measures are useful for *in situ* calibration of surface reflectance for terrestrial imaging spectroscopy studies.

Site Name	Coordinates (Average)		Altitude (m a.s.l.)
	Latitude (North)	Longitude (East)	
M1	38.40620	14.96105	331
M2	38.38553	14.96100	330
M3	38.40617	14.96080	325
M4	38.40601	14.96043	325
M5	38.40606	14.96037	323
M6	38.40591	14.95997	331
M7	38.40595	14.96002	333
M8	38.40585	14.95997	324
M9	38.40585	14.95981	336
M10	38.40568	14.95971	320
M11	38.40583	14.95991	324
M12	38.40477	14.95938	322
M13	38.40488	14.95930	342
M14	38.40414	14.95916	325
M15	38.40388	14.95943	342
M16	38.40401	14.95952	323
M17	38.40399	14.95876	351
M18	38.40320	14.95886	374
M19	38.40315	14.95889	374
M20	38.40250	14.95989	399
M21	38.40244	14.95991	395
M22	38.40191	14,96223	400
M23	38.40192	14.96221	402
M24	38.40246	14.96461	406
M25	38.40295	14.96492	422
M26	38.40646	14.95835	280
M27	38.40645	14.95830	279

Table 2. First day: GPS coordinates of the selected points and number of measurements collected by ASD-fieldSpec.

In Figure 32, Figure 33 and Figure 34 examples of mean values of reflectance measured in three different sites during the first day of measurements are reported. In particular, in Figure 34 it is evident how the presence of vegetation can influence the spectra characterization. In the figures a noisy reflectance usually occurred in the area ranges from 1350 to 1410 nm and from 1800 to 2000 nm due to atmospheric interference.

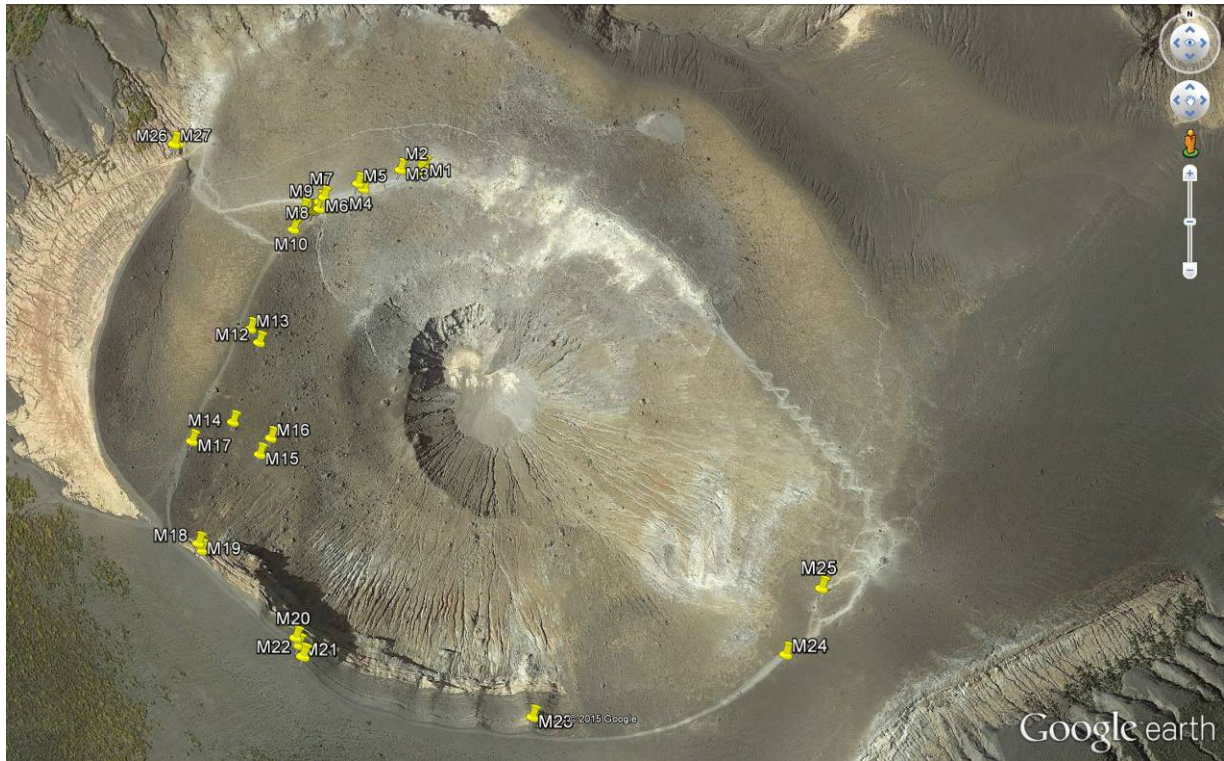


Figure 31. First day: measurement points acquired with ASD-FieldSpec.

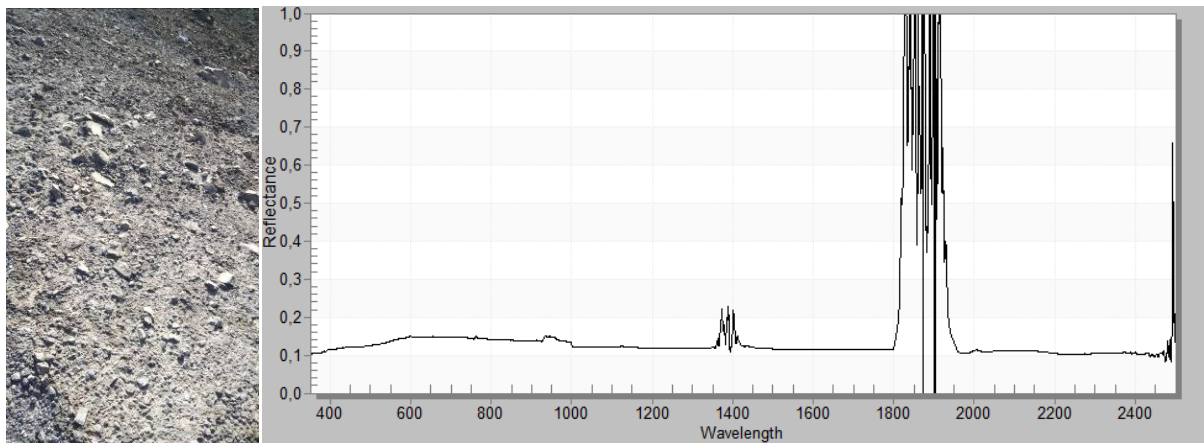


Figure 26. Reflectance spectrum acquired on site M4.

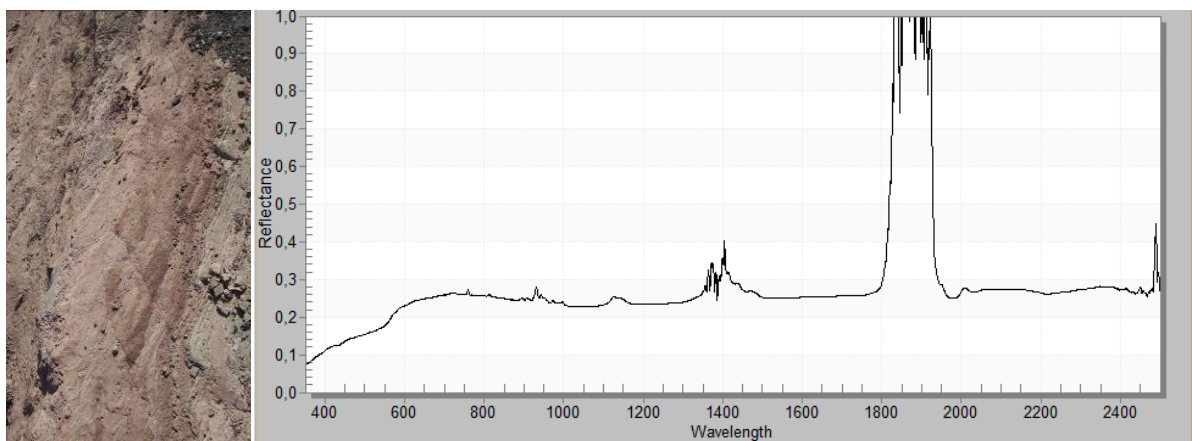


Figure 27. Reflectance spectrum acquired on site M18.

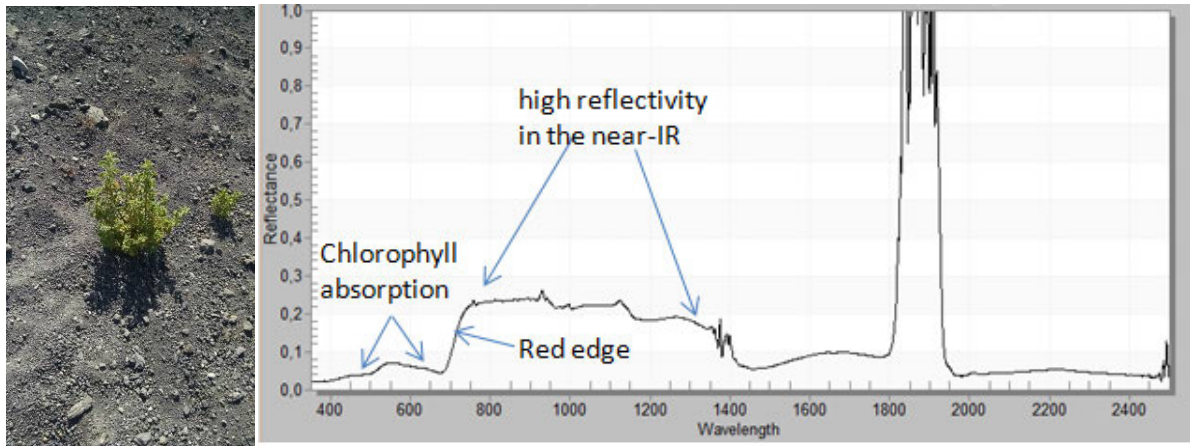


Figure 28. Reflectance spectrum acquired on site M22. In the near infrared wavelengths (700-1400 nm) it is evident the presence of vegetation, characterized by typical curve.

On 4th September reflectances values were measured also in the “Pozza dei fanghi” area (Figure 35 and Table 3).

Site Name	Coordinates (Average)		Altitude (m)
	Latitude (North)	Longitude (East)	
M1	38.41631	14.95948	56
M2	38.41631	14.95952	43
M3	38.41633	14.95959	42
M4	38.41619	14.95995	40
M5	38.41607	14.96001	43
M6	38.41605	14.96006	48
M7	38.41575	14.96005	53
M8	38.41573	14.96003	50
M9	38.41573	14.96022	51
M10	38.41570	14.96021	53
M11	38.41595	14.96056	59
M12	38.41595	14.96046	60
M13	38.41657	14.95959	49
M14	38.41656	14.95965	39
M15	38.41699	14.95945	43

Table 3. Second day: GPS coordinates of the selected points and number of measurements collected by ASD-fieldSpec.

In Figure 36, Figure 37 and Figure 38 examples of mean reflectance values measured in three different sites of this area are reported.



Figure 29. Second day: measurement points acquired with ASD-FieldSpec at the “Pozza dei fanghi” area.

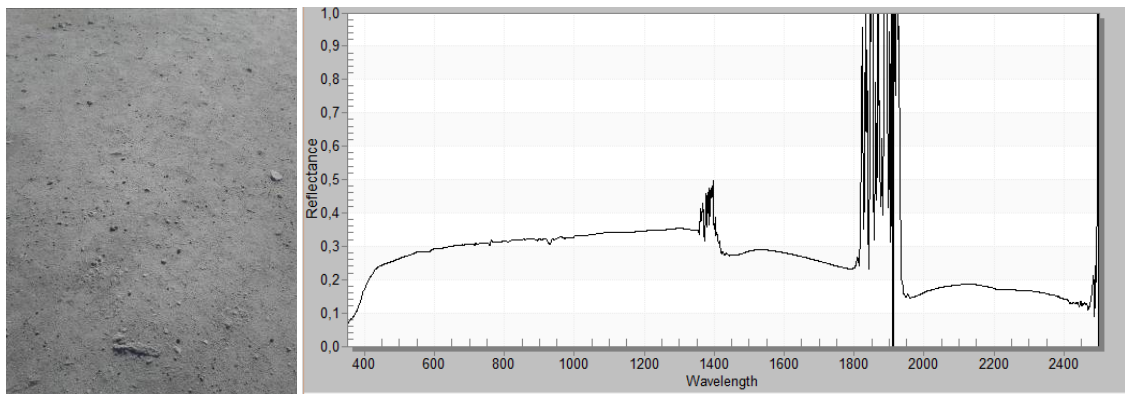


Figure 30. Reflectance spectrum acquired on site M2.

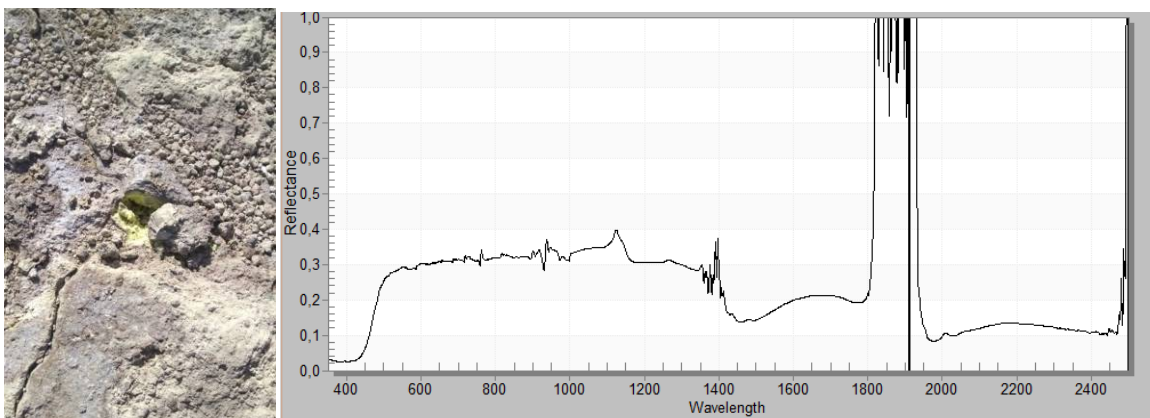


Figure 31. Reflectance spectrum acquired on site M8.

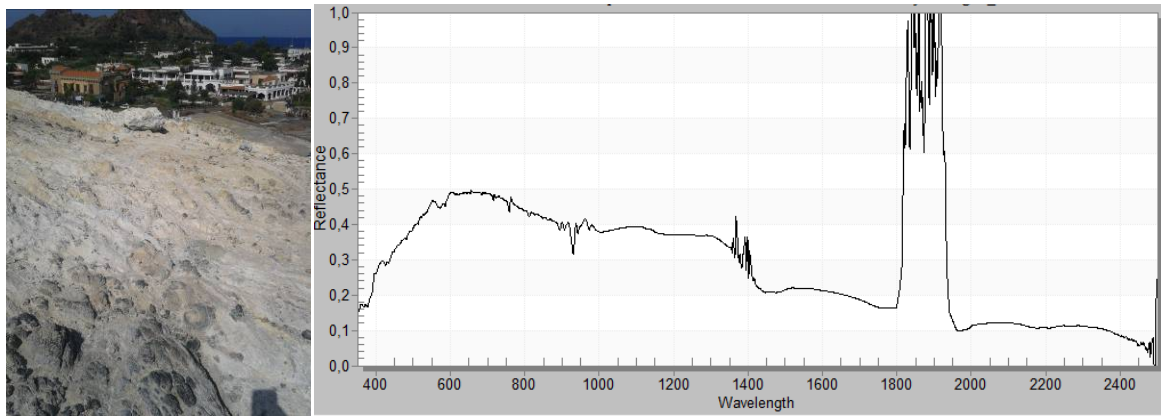


Figure 32. Reflectance spectrum acquired on site M12.

On 6th September reflectances values were collected according to the ASTER satellite crossing on 6th of September 2015 at about 10.00 UTM (Figure 39 and Table 4), even if at the ASTER acquisition time the weather was cloudy and the measurements with the spectroradiometer were collected not during the period of the satellite overpass but later when the sky was clear.

Site Name	Coordinates (Average)		Altitude (m)
	Latitude (North)	Longitude (East)	
M1	38.41986	14.95709	51
M2	38.41992	14.95708	40
M3	38.41981	14.95709	10
M4	38.42009	14.95678	0
M5	38.41943	14.95699	0
M6	38.41898	14.95624	0
M7	38.41546	14.96183	46
M8	38.41547	14.96176	40
M9	38.41553	14.96092	40
M10	38.41548	14.96050	41
M11	38.41547	14.96038	40

Table 4. Third day: GPS coordinates of the selected points and number of measurements collected by ASD-fieldSpec.

In Figure 40 and Figure 41 example of reflectance collected are reported.



Figure 33. Third day: measurement points acquired with ASD-FieldSpec.

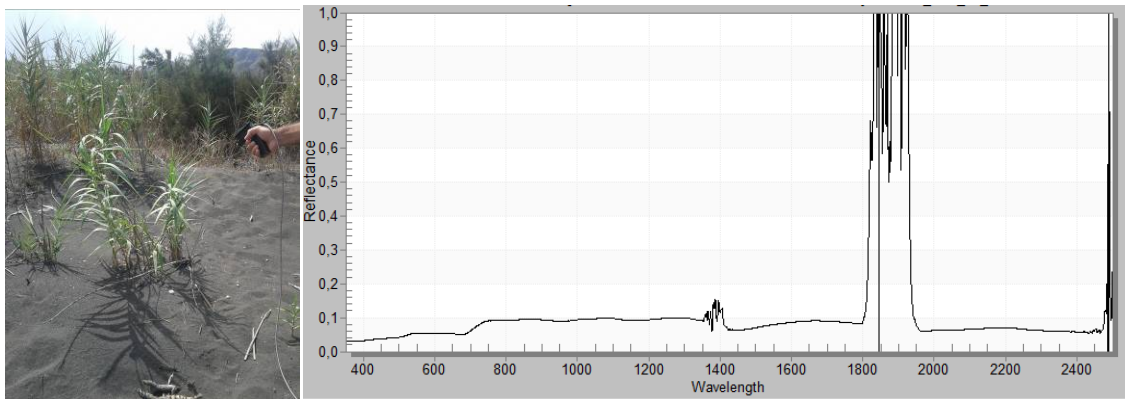


Figure 40. Reflectance spectrum acquired on site M3.

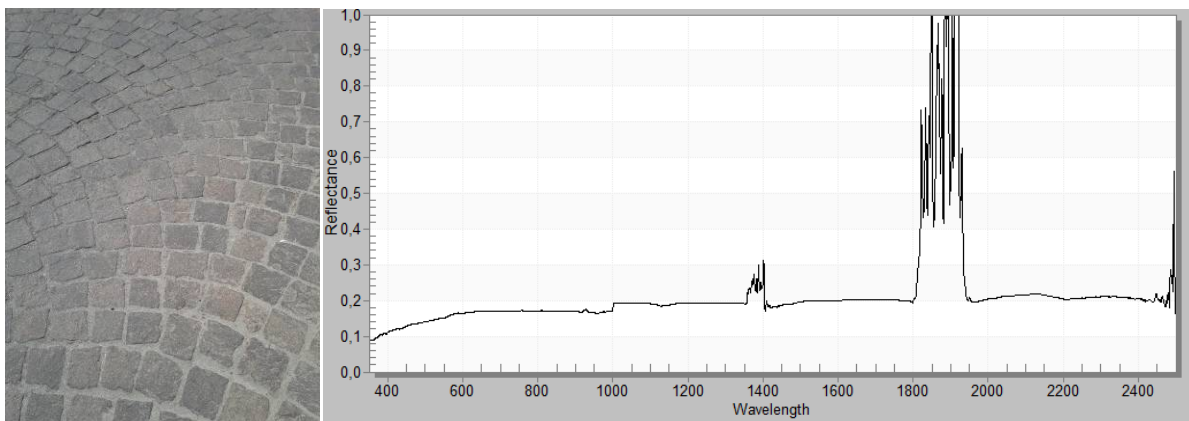


Figure 41. Reflectance spectrum acquired on site M11.

3. Satellite data

During the Vulcano Island field campaign, two sets of satellite data were considered: those from Landsat 8 and those from ASTER. Unfortunately during the day of ASTER acquisition, the sky was cloudy over the island. For this reason the ASTER data could not be analyzed (Figure 42). All the images have been released by providers.

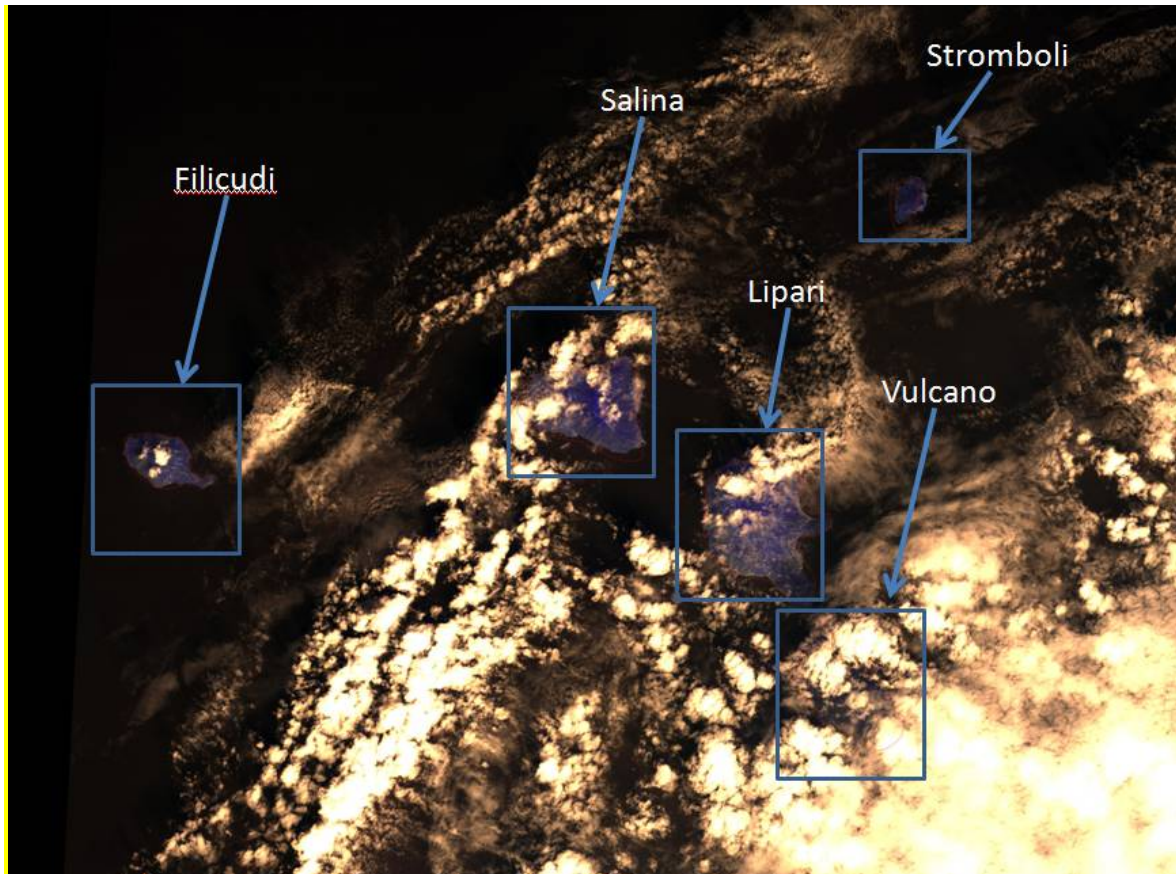


Figure 34. RGB image of ASTER data acquired on 6th September, showing the cloud cover over Vulcano Island.

3.1 Landsat 8 data

The Landsat 8 satellite collects images of the entire Earth every 16 days with an 8-day offset from Landsat 7. The Landsat 8 satellite of the Landsat Data Continuity Mission was launched by the National Aeronautics and Space Administration (NASA) in April 2013. The satellite is endowed with two earth-observation sensors: the Operational Land Imager (OLI) and the Thermal Infrared Sensor (TIRS). OLI has spectral bands ranging from visible to shortwave, whereas TIRS has two thermal infrared bands for Earth-emitted electromagnetic signal detection (band 10, 10.60–11.19 μm and band 11, 11.50 - 12.51 μm). For surface temperature the TIRS sensor is normally used. Data are delivered in quantized and calibrated scaled Digital Numbers (DN) representing multispectral image. The band 10 data were automatically extracted using ENVI and IDL software and were converted to top of atmosphere (TOA) radiance (L_{TOA} , $\text{W}\cdot\text{m}^{-2}\cdot\text{sr}^{-1}\cdot\mu\text{m}^{-1}$) with the following equation:

$$L_{\text{TOA}} = \text{ML} Q_{\text{cal}} + \text{AL} \quad (1)$$

Where:

ML is the multiplicative rescaling factor (3.342×10^{-4}) for Landsat-8 band 10 metadata, from the MTL file furnished with the image data;

Q_{cal} is the quantized and calibrated standard digital pixel number (DN) value;
 AL is the additive rescaling factor (0.1) for Landsat-8 band 10 metadata, from the MTL.

To estimate the surface temperature, the band 10 TOA spectral radiance was computed and used in conjunction with the Modtran radiative transfer model for atmospheric corrections, obtaining the at surface spectral radiance at the surface (L_λ).

Using these data, the spectral radiance leaving the emitting surface at temperature T (K) (L_λ , $W \cdot m^{-2} \cdot sr^{-1} \cdot \mu m^{-1}$) could be calculated by rearranging the following equation from Barsi et al., [2005]:

$$L_{TOA} = \tau \varepsilon L_\lambda + L_u + \tau(1-\varepsilon) L_d \quad (2)$$

where:

L_{TOA} is the TOA radiance received by band 10 of the sensor with brightness temperature T_{10} ;

L_λ is the radiance from the surface at band 10;

L_u is the upwelling atmospheric radiance components (obtained using Modtran);

L_d is the downwelling atmospheric radiance components (obtained using Modtran);

ε is the surface emissivity for band 10 extracted by the ASTER 05 emissivity data;

τ is the atmospheric transmittance for band 10 when view zenith angle is θ (obtained using Modtran).

TIRS is treated as nadir viewing since the view angle is no more than 7.5° .

The radiance at sensor (L_{TOA}) has been corrected for the atmospheric effect in order to obtain the radiance emitted by the surface (L_λ) using the Modtran radiative transfer model. For these data we have considered the ‘‘CIRILLO’’ atmospheric correction tools [Musacchio et al., 2007]. Information on the atmospheric profiles corresponding in time to the Landsat overflights were provided by the University of Wyoming. Atmospheric temperature, pressure and humidity at the time of Landsat overflights were also considered.

Since the surface emissivity is known from ASTER 05 data, it was possible to correct the values of L_{TOA} for the reflected sky radiation in Eq (2) and inverting Planck’s equation to get the surface temperature.

TIRS band data can be converted from spectral radiance to temperature using the thermal constants provided in the metadata file (the MTL file furnished with the image data) and applying the formula:

$$T = K_2 / (\ln (K_1 / L_\lambda + 1)) \quad (3)$$

where

T is the surface temperature ($^\circ K$);

L_λ is the surface spectral radiance;

K_1 is the Band-specific thermal conversion constant contained in the MTL file;

K_2 is the Band-specific thermal conversion constant contained in the MTL file;

Details about Landsat 8 TIRS stray light can be found in the Landsat 8 Data Users Handbook [U.S.G.S. Landsat User Services, 2016].

In Figure 43 the surface temperature for the 5th September 2015 survey is shown. It is possible to note that the image acquired during the daytime has its shortwave infrared observations contaminated by reflected solar radiation, therefore the apparent surface temperature is higher than the real one. During the nighttime this contamination is not present and the obtained temperature has acceptable values.

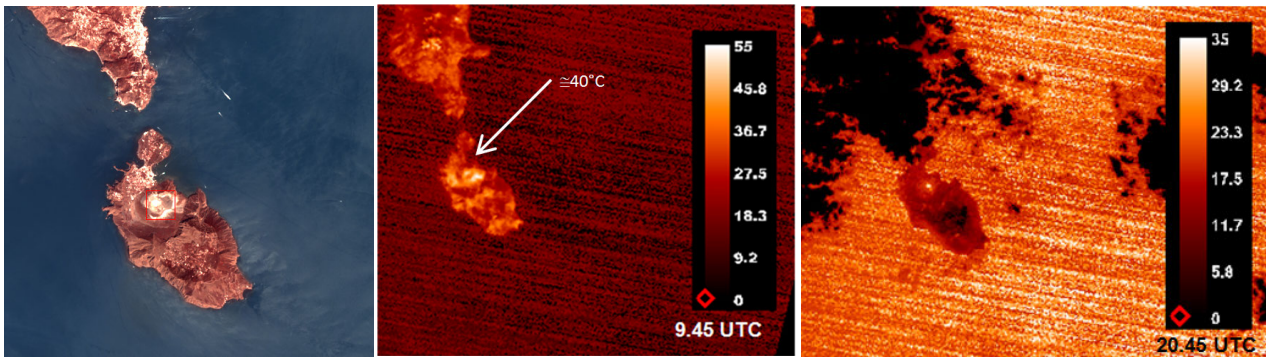


Figure 35. RGB Landsat 8 image (left) using the first three channels with spatial resolution of 30m, surface temperature on 5 September (daytime - center), surface temperature on 5 September (night-time - right). The temperature is in degree Celsius. The arrow plotted in the center indicates the “Pozza dei fanghi” area.

Considering the ground temperature measurements acquired by using the thermal camera (Figure 29) and the one obtained using the Landsat 8 data, showed in Figure 43, the values are comparable. In fact the mean land temperature of the “Pozza dei fanghi” area at Vulcano measured on 5th September is around 40°C.

Conclusions

The present work had the goal of describing the testing of new small, economical UAV platforms, with miniaturized instrument payloads, within fumaroles of active Italian volcanoes. With such technology, in situ and proximal remote sensing measurements of volcanic plumes are now possible without risking the lives of scientists and personnel in charge of close monitoring of volcanic activity. Previous versions of the miniGAS payload and portable mass spectrometer instrument were already used in the Costa Rica at Turrialba Volcano [Diaz et al., 2010; Pieri et al., 2013] and Solfatara volcano [Silvestri et al., 2015, Diaz et al., 2015; Wright and Diaz, 2015]. The updated NTX and UAS-MS versions were fully tested by the INGV volcanologists during the 2015 Solfatara and Vulcano campaigns, providing important feedback on their operation and indicating their limitations. The systematic collection of in situ data regarding volcanic plume parameters (e.g., temperature, pressure, relative humidity and SO₂ concentration) offers a valid support to the calibration and validation of remote sensing imagery and to the monitoring of volcanic activity and/or research.

Moreover the campaign provided a positive result in terms of verifying the instrument portability in areas without easy access. Some considerations can be done by analyzing the obtained results on the instruments used. The first concerns T-Guard: the membrane can be easily destroyed due to acidic gases, so an acid filter need to be incorporated into the intake line for the next campaigns. A second consideration concerns the UAS-MS MPH system and the developing of a future version of its FabGuard® so as to compensate for oxygen depletion with real time data analysis and design of the probe to be inserted directly into the fumarole.

Concerning the SO₂ measurements using LP-DOAS, new campaigns will be planned to repeat the field measurements with a different optical setup, enhancing the UV source in the strongest differential absorption lines of chemical species.

The Solfatara and Vulcano campaigns have been organized taking into account the two scheduled reference satellite acquisitions: TERRA ASTER and LANDSAT8. Both satellite data have been used to compare the satellite measurements with the *in situ* measurements, particularly as regards temperature.

According to the schedule, the TERRA-ASTER daytime image of September 6 and the LANDSAT 8 images of September 5 (both daytime and nighttime) were acquired. Only the acquired LANDSAT 8 images were cloud free. Despite the ASTER data were not used, in order to support the analysis of exploited instruments, surface spectra reflectance has been acquired by means of ground portable instruments. Considering the spatial and temporal low seasonal variability these data will be used for reanalyzing future collected ASTER data.

The land surface temperature measured by satellite is quite comparable with the one acquired by thermal camera and the discrepancies between observed and modeled temperatures are principally due to

several factors such the difference of spatial resolution of satellite data and the “point-size” ground observations.

Finally this campaign provided a huge volume of data whose interpretation and comparison with different methodologies (collected on site and derived by satellite) is out of the scope of this report, but that will be thoroughly analyzed in an following study.

Acknowledgements

We want to thank all colleagues for their hospitality, and the great support provided during the visit of foreign colleagues during the field campaigns at Solfatara and at Vulcano Island.

In particular we thank to Stefano Caliro and all the staff of the laboratory that allowed Prof. Andres Diaz to assemble and calibrate his equipment, the Rete Mobile of Centro Nazionale Terremoti and Milena Moretti for providing technical equipment in support of the campaigns. We thank all the groups who helped us with the different measures to complete the test and especially Salvatore Inguaggiato, Paolo Madonia and Marianna Cangemi.

Special thanks is given to Dr. David Pieri, ASTER science Team Member, for the data acquisition planning support and to the Jet Propulsion Laboratory, California Institute of Technology for providing ASTER imagery.

We would like to thank our colleagues Iacopo Nicolosi and Roberto Carluccio from INGV Section of Roma 2, for sharing their huge experience in the drone piloting, assembling and related security and to Massimo Chiappini Director of INGV Section of Roma 2 for lending their drones and many instruments from their laboratory.

Finally we thank Alessio Buonomo for the photographic material collected during the measurement campaign and his precious support in the campaigns and Serena Tramonti for her English support.

References

- Aiuppa A., Tamburello G., Di Napoli R., Cardellini C., Chiodini G., Giudice G., Grassa F., Pedone M., (2013). *First observations of the fumarolic gas output from a restless caldera: Implications for the current period of unrest (2005–2013) at Campi Flegrei*. *Geochem. Geophys. Geosys.* doi: 10.1002/ggge.20261 ISSN: 1525-2027.
- Barsi J.A., Schott J.R., Palluconi F.D., Hook S.J., (2005). *Validation of a web-based atmospheric correction tool for single thermal band instruments*. *Proc. SPIE.* doi:10.1117/12.619990.
- Bogumil K., Orphal J., Homann T., Voigt S., Spietz P., Fleischmann O.C., Vogel A., Hartmann M., Kromminga H., Bovensmann H., Frerick J., Burrows J.P., (2003). *Measurements of molecular absorption spectra with the SCIAMACHY pre-flight model: instrument characterization and reference data for atmospheric remote-sensing in the 230-2380 nm region*. *J. Photoch. Photobio. A*, 157, 167-184.
- Colini L., Spinetti C., Amici S., Buongiorno M.F., Caltabiano T., Doumaz F., Favalli M., Giammanco S., Isola I., La Spina A., Lombardo V., Mazzarini F., Musacchio M., Neri M., Salerno G., Silvestri M., Teggi S., Sarli V., Cafaro P., Mancini M., D’Andrea S., Curci G., Ananasso C., (2014). *Hyperspectral spaceborne, airborne and ground measurements campaign on Mt. Etna: multi data acquisitions in the frame of Prisma Mission (ASI-AGI Project n. I/016/11/0)*. *Quaderni di Geofisica*, n. 119.
- Diaz J.A., Pieri D., Arkin R., Gore E., Griffin T.P., Fladeland M., Bland G., Soto C., Madrigal Y., Castillo D., Rojas E., Achi S., (2010). *Utilization of in situ airborne MS-based instrumentation for the study of gaseous emissions at active volcanoes*. *International Journal of Mass Spectrometry*, 295, 105 – 112. doi:10.1016/j.ijms.2010.04.013.
- Diaz J.A., Pieri D., Wright K., Sorensen P., Kline-Shoder R., Arkin C.R., Fladeland M., Bland G., Buongiorno M.F., Ramirez C., Corrales E., Alan A., Alegria O., Diaz D. and Linick J., (2015). *Unmanned aerial mass spectrometer systems for in-situ volcanic plume analysis*. *J. Am. Soc. Mass. Spectrom.* 26(2): 292-304. doi: 10.1007/s13361-014-1058-x. Epub 2015 Jan 15.
- Kern C., Trick S., Rippel B., Platt U., (2006). *Applicability of light-emitting diodes as light sources for active differential optical absorption spectroscopy measurements*. *Appl. Opt.* 45:2077-2088.
- Galle B., Johansson M., Rivera C., Zhang Y., Kihlman M., Kern C., Lehmann T., Platt U., Arellano S.,

- Hidalgo S., (2010). *Network for Observation of Volcanic and Atmospheric Change (NOVAC) - A global network for volcanic gas monitoring: Network layout and instrument description*. J. Geophys. Res. 115:D05304. doi:10.1029/2009JD011823.
- Holben B.N., Tanré D., Smirnov A., Eck T.F., Slutsker I., Abuhassan N., Newcomb W.W., Schafer J., Chatenet B., Lavenue F., Kaufman Y.J., Vande Castle J., Setzer A., Markham B., Clark D., Frouin R., Halthore R., Karnieli A., O'Neill N.T., Pietras C., Pinker R.T., Voss K., Zibordi G., (2001). *An emerging ground-based aerosol climatology: aerosol optical depth from AERONET*. J. Geophys. Res. 106 (D11), 12,067–12,097. doi:10.1029/2001JD900014.
- Landsat 8 Data User Handbook. <http://landsat.usgs.gov/documents/Landsat8DataUsersHandbook.pdf>
- Musacchio M., Amici S., Silvestri M., Teggi S., Buongiorno M.F., Silenzi S., and Devoti S., (2007). *Application of CIRILLO a new atmospheric correction tool on Castel Porziano Beach (CPB)*. Proc. SPIE 6749, Remote Sensing for Environmental Monitoring, GIS Applications, and Geology VII, 674935 (October 30, 2007). doi:10.1117/12.752670.
- Musacchio M., Doumaz F., Favalli M., Nedjari A., Maouche S., Rahil M., (2015). *Preliminary activity for identification and characterization of an international CAL/VAL site*. Rapporti Tecnici INGV, ISSN 2039-7941, n. 329.
- Pieri D., Diaz J.A., Bland G., Fladeland M., Madrigal Y., Corrales E., Alegria O., Alan A., Realmuto V., Miles T. and Abtahi A., (2013). *In situ observations and sampling of volcanic emissions with NASA and UCR unmanned aircraft, including a case study at Turrialba Volcano, Costa Rica*. The Geological Society of London, Special Publications, 380, 321-352. <http://dx.doi.org/10.1144/SP380.13>.
- Platt U., (1994). *Differential optical absorption spectroscopy (DOAS)*. Chem. Anal. Series, 127, 27 - 83.
- Platt U. and Perner D., (1983). *Measurements of atmospheric trace gases by long path differential UV/visible absorption spectroscopy*. D.A. Killinger and A. Mooradian (eds.), Optical and Laser Remote Sensing, Springer Verlag, New York, 95-105.
- Platt U., Stutz J., (2008). *Differential Optical Absorption Spectroscopy Principles and Applications*. Physics of Earth and Space Environments. Springer.
- Porter J.N., Horton K.A., Mouginis-Mark P.J., Linert B., Shiv K. Sharma, Lau E., Sutton A.J., Elias T., Oppenheimer C., (2002). *Sun photometer and lidar measurements of the plume from the Hawaii Kilauea Volcano Pu'u O'o vent: Aerosol flux and SO₂ lifetime*. Geophysical Research Letters, 29, 16, 10.1029/2002GL014744, 2002.
- Silvestri M., Diaz J.A., Marotta E., Musacchio M., Buongiorno M.F., Sansivero F., Cardellini C., Pieri D., Amici S., Bagnato E., Beddini G., Belviso P., Carandente A., Colini L., Doumaz F., Peluso R., Spinetti C., (2015). *Use of multiple in situ and remote sensing instruments and techniques at solfataro field campaign for measurements of CO₂, H₂S and SO₂ emissions: special demonstration on unmanned aerial systems*. Quaderni di Geofisica, n. 129.
- U.S.G.S. Landsat User Services (2016). *Landsat 8 (L8) Data Users Handbook*, LSDS - 1574, vers. 2.0, EROS, Sioux Falls, 106 pp., <http://landsat.usgs.gov/documents/Landsat8DataUsersHandbook.pdf>
- Vita F., Inguaggiato S., Bobrowski N., Calderone L., Galle B., Parello F., (2012). *Continuous SO₂ flux measurements for Vulcano Island, Italy*. Annals of Geophysics, 55, 2, 2012; doi: 10.4401/ag-5759.
- Vita F., Kern C. and Inguaggiato S., (2014). *Development of a portable active long-path differential optical absorption spectroscopy system for volcanic gas measurements*. J. Sens. Sens. Syst., 3, 355-367, doi:10.5194/jsss-3-355-2014.
- Watson I.M. and Oppenheimer C., (2001). *Photometric observations of Mt. Etna's different aerosol plumes*. Atmospheric Environment, 35, 3561-3572.
- Wright K. and Diaz J.A., (2015). *In-situ Volcanic Plume Monitoring at Solfataro Volcano and Vulcano Island, Italy with Small Portable Mass Spectrometer Systems designed for Field Deployment and Unmanned Aerial Vehicles (UAV)*. 10th Workshop on Harsh-Environment Mass Spectrometry. September 13–16, 2015, Baltimore.

Sitografia

<http://fsf.nerc.ac.uk/instruments/sunphotometer.shtml>

Quaderni di Geofisica

ISSN 1590-2595

<http://istituto.ingv.it/l-ingv/produzione-scientifica/quaderni-di-geofisica/>

I Quaderni di Geofisica coprono tutti i campi disciplinari sviluppati all'interno dell'INGV, dando particolare risalto alla pubblicazione di dati, misure, osservazioni e loro elaborazioni anche preliminari, che per tipologia e dettaglio necessitano di una rapida diffusione nella comunità scientifica nazionale ed internazionale. La pubblicazione on-line fornisce accesso immediato a tutti i possibili utenti. L'Editorial Board multidisciplinare garantisce i requisiti di qualità per la pubblicazione dei contributi.

Rapporti tecnici INGV

ISSN 2039-7941

<http://istituto.ingv.it/l-ingv/produzione-scientifica/rapporti-tecnici-ingv/>

I Rapporti Tecnici INGV pubblicano contributi, sia in italiano che in inglese, di tipo tecnologico e di rilevante interesse tecnico-scientifico per gli ambiti disciplinari propri dell'INGV. La collana Rapporti Tecnici INGV pubblica esclusivamente on-line per garantire agli autori rapidità di diffusione e agli utenti accesso immediato ai dati pubblicati. L'Editorial Board multidisciplinare garantisce i requisiti di qualità per la pubblicazione dei contributi.

Miscellanea INGV

ISSN 2039-6651

<http://istituto.ingv.it/l-ingv/produzione-scientifica/miscellanea-ingv/>

La collana Miscellanea INGV nasce con l'intento di favorire la pubblicazione di contributi scientifici riguardanti le attività svolte dall'INGV (sismologia, vulcanologia, geologia, geomagnetismo, geochimica, aeronomia e innovazione tecnologica). In particolare, la collana Miscellanea INGV raccoglie reports di progetti scientifici, proceedings di convegni, manuali, monografie di rilevante interesse, raccolte di articoli ecc..

Coordinamento editoriale e impaginazione

Centro Editoriale Nazionale | INGV

Progetto grafico e redazionale

Daniela Riposati | Laboratorio Grafica e Immagini | INGV

© 2016 INGV Istituto Nazionale di Geofisica e Vulcanologia

Via di Vigna Murata, 605

00143 Roma

Tel. +39 06518601 Fax +39 065041181

<http://www.ingv.it>



Istituto Nazionale di Geofisica e Vulcanologia